miRNome profiling reveals differential miRNAs associated with embryogenic potential in the somatic embryogenesis of Araucaria angustifolia

Leandro Francisco de Oliveira (lfdeoliveira@usp.br)
Universidade de Sao Paulo https://orcid.org/0000-0002-5318-2771
Amanda Rusiska Piovezani
Universidade de São Paulo: Universidade de Sao Paulo
Eny Iochevet Segal Floh
Universidade de São Paulo: Universidade de Sao Paulo

Research Article

Keywords: Brazilian pine, miRNAs, post-transcriptional regulation, somatic embryos

Posted Date: March 21st, 2023

DOI: https://doi.org/10.21203/rs.3.rs-2626215/v1

Version of Record: A version of this preprint was published at Plant Cell, Tissue and Organ Culture (PCTOC) on July 26th, 2023. See the published version at https://doi.org/10.1007/s11240-023-02576-6.

Abstract

Somatic embryogenesis occurs through complex processes modulated by gene regulatory networks at an appropriate spatiotemporal scale important for cell division and differentiation. Post-transcription regulation mechanisms mediated by miRNAs control the expression of several genes involved in embryogenesis. Transcript and proteomics studies in embryogenic cultures from *Araucaria angustifolia*, an endangered native Brazilian conifer with ecological and economic importance, have indicated a role for post-transcriptional regulation in this process. One example is the differential abundance of ARGONAUTE between two contrasting embryogenic cell lines. Here, we profiled the miRNA expression pattern in two cell lines of *A. angustifolia* with distinct embryogenic potential using small RNA sequencing technology. We identified 165 mature miRNAs, of which 143 were novel and 22 were conserved plant miRNAs. Seven miRNA conserved families were identified: miR156, miR169, miR394, miR482, miR536, miR1030, and miR1314. Most miRNAs were differentially expressed during the transition from proliferation to the maturation stage of somatic embryogenesis, suggesting that miRNAs play more important roles in the early somatic embryo development. A total of 98 potential target genes were found for 89 miRNAs, involved in post-transcriptional processes, transporters, defense response, sugar regulation, stress, ABA controlling and signaling, cell-to-cell communication, maintaining suspensor cell identity, brassinosteroids signaling, and cell division. Negative correlations of expression patterns between miRNAs and their targets were detected for miR1030-*PRL1*, miR1314-*ADR1-Like*, and Aang34-*LRR* modules, when analyzed by RT-qPCR. Taken together, our findings provide new insights into the regulatory roles of miRNAs and their target genes in the somatic embryogenesis of Brazilian pine.

Introduction

Plant embryogenesis is controlled by complex gene regulatory networks that regulate spatiotemporal transcription and translation during cell division and differentiation (Sparks et al. 2013; Navarro et al. 2017; Juárez-González et al. 2019). Accessing the early stages of the zygotic embryo is challenging, therefore, somatic embryogenesis has been used as a model to study how this process is regulated at the molecular level (Rodrigues et al. 2019). The required conditions and regulatory programs of somatic embryogenesis vary between plant species (Juárez-González et al. 2019). Somatic embryogenesis is also considered a biotechnological tool used as a clonal propagation technology in several conifer species in which somatic embryos are induced mainly from immature and mature zygotic embryos (Rodrigues et al. 2019).

While somatic embryogenesis protocols have been successfully established for many conifers, several drawbacks exist for *Araucaria angustifolia* (Brazilian pine), an endangered species found in southern Brazil. Due to intense exploration in the past century, current populations cover less than 2% of their original forest area (Jo et al. 2014; de Oliveira et al. 2020). *A. angustifolia* is an interesting non-model species that belongs to Araucariaceae, a basal family among Coniferophyta species (Durzan 2012; Elbl et al 2022), which provide valuable information on evolutionary plant embryo development. Until now, its complete embryogenesis was not achieved and only a few cotyledon somatic embryos have been obtained (dos Santos et al. 2016; de Oliveira et al. 2018). Part of this limitation is due to a poor understanding of the underlying genetic programs and biochemical pathways that regulate embryogenesis in this species (de Oliveira et al. 2017).

To tackle this bottleneck, different molecular and biochemical studies using comparative transcriptomics, proteomics, and metabolism pathways have been performed in *A. angustifolia* (Jo et al. 2014; Elbl et al. 2015a; dos Santos et al. 2016; Navarro et al. 2017; de Oliveira et al. 2017, 2018, 2020; Elbl et al. 2022). dos Santos et al. (2016) carried out a proteomic comparison between two *A. angustifolia* distinct cell lines with different potential to develop somatic embryos: an embryo forming (Responsive) and a non-embryo forming (Blocked) cell lines. A putative member of the ARGONAUTE (AGO) family was found to be more abundant in the Responsive compared to the Blocked cell line. AGO together with microRNAs (miRNAs) and other proteins form so-called RNA-induced silencing complexes (RISCs) (Zhang et al. 2018a,b). RISCs carrying miRNAs are responsible to regulate target mRNAs and have been associated with the correct development of zygotic and somatic embryos in conifers, including *A. angustifolia* (Tahir et al. 2006; Schlögl et al. 2012a, b). Conversely, a putative glycine-rich RNA-binding protein 7 (GRP7) was more abundant in the Blocked cell line (dos Santos et al. 2016). This protein is involved in primary miRNA transcript (pri-miRNA) processing (Streinter et al. 2012), and its overexpression altered miRNA composition in cells of *A. thaliana* (Köster et al. 2014). These findings suggest a misbalance in transcript composition between the two contrasting cell lines, which could be associated with the loss of maturation competence in the Blocked cell line (dos Santos et al. 2016).

Gene expression is regulated at both transcriptional and post-transcriptional levels to ensure the correct regulation of plant growth and development (Wei et al. 2018; Jeena et al. 2022). The plant gene silencing process is mediated by small non-coding classes of RNAs,

including miRNAs and small interfering RNA (siRNAs) (Lakhwani et al. 2020). miRNAs are a distinct class of single-stranded RNA of ~ 18–25 nucleotides (Zhang et al. 2018a,b; Lin et al. 2020). *MIR* genes are endogenously transcribed as long precursor transcripts (pri-miRNAs), forming a fold-back hairpin structure with the small RNA embedded in one of its arms (Rogers and Chen 2013; Chorostecki et al. 2017). MiRNAs play a key role in post-transcriptional regulation or repression of translation mechanisms (Tiwari et al. 2020). The mature miRNAs negatively regulate gene expression by binding to the partially complementary sequences in the target messenger RNAs (mRNAs), in their opening reading frame (ORF) or UTR regions of specific target genes (Zhang et al. 2018a; Liu et al. 2019). Then, cleavage and degradation of mRNA molecules or inhibition of translation are carried out with the cooperation of RISC (Liu et al. 2019).

Over hundreds miRNA targets seem to be expressed in the developing embryo underlining the relevant role of miRNAs in embryogenesis (Alves et al. 2020; Jeena et al. 2022). Identifying the miRNAs that regulate somatic embryogenesis extends our knowledge about the regulatory pathways controlling embryogenic transitions (Wójcik et al. 2017; Juárez-González et al. 2019; Siddiqui et al. 2019), with implications for control of cell-specific gene expression programs according to both spatial and temporal cues (Plotnikova et al. 2019). The proper patterning and morphology of embryos are related to the expression of miRNAs and their targets (Wójcik et al. 2016; Siddiqui et al. 2019) in different plant systems: *Citrus sinensis* (Wu et al. 2011), *Larix leptolepis* (Zhang et al. 2013), *Picea balfouriana* (Li et al. 2017), *Pinus pinaster* (Rodrigues et al. 2019), and *Dimocarpus longan* (Xu et al. 2020).

Until now, 8,615 precursor miRNAs and 10,414 mature miRNAs have been detected in Viridiplantae (http://www.mirbase.org, release 22.1, Kozomara et al. 2019). From these, 662 and 669 were shown to be precursor and mature sequences, respectively, from four conifer species: *Cunninghamia lanceolata*, *Picea abies*, *Pinus densata*, and *Pinus taeda.* However, information on miRNAs in the Araucariaceae family is still missing.

This work complements our previous proteome and transcriptome studies on *A. angustifolia* (Elbl et al. 2015a; dos Santos et al. 2016) investigating for the first time the miRNA-associated regulation of somatic embryogenesis. We employed high-throughput paired RNA-sequencing to identify conserved and novel miRNAs and their targets involved in *A. angustifolia* somatic embryo development. Our results pave the way for a better understanding of the gene expression regulation during somatic embryogenesis development.

Material And Methods

Plant material and experimental conditions

Embryogenic cell lines previously induced from *A. angustifolia* immature zygotic embryos (de Oliveira et al. 2018, 2020) were used in this study. Two cell lines were selected based on their capacity to form somatic embryos under maturation conditions (described below). Cell lines were classified as described by Jo et al. (2014) and resulted in: (i) Blocked cell line (Fig. 1A) incapable of developing somatic embryos in the maturation medium (Fig. 1B); or (ii) Responsive (Fig. 1C), i.e., cells capable of producing early somatic embryos in the maturation conditions (Fig. 1D). The two cell lines are similar in the dynamic growth (fresh and dry weight), as well as reaching the lag, exponential, linear, and stationary phases at the same time after transfer to fresh medium, as described by de Oliveira et al. (2018).

Two stages of *A. angustifolia* somatic embryogenesis protocol were considered in this study, proliferation and maturation (Fig. 1). For the proliferation stage, pro-embryogenic masses (PEMs) were grown on a semi-solid MSG medium (Becwar et al. 1989), pH 5.8, containing 1.46 $g.l^{-1}$ L-glutamine, 3% (w/v) sucrose, and 0.3% (w/v) Gelrite® and harvested after two weeks. For the maturation stage, PEMs were collected from the surface callus after 14 days of growth in the proliferation conditions and dissociated into MSG liquid culture medium at a ratio of 1:20 (w/v). One milliliter of the cell suspension (containing 50 mg FW PEMs) was transferred to filter paper (Whatman® No. 1, 70 mm) containing 25 ml of MSG-maturation medium in Petri dishes (100 × 15 mm). The maturation medium was constituted by MSG medium, pH 5.8 supplemented with 3% (w/v) sucrose, 3% (w/v) sorbitol, 1.46 $g.l^{-1}$ L-glutamine, 1% (w/v) Gelrite®, and 120 µM of abscisic acid (ABA). The cultures grown in the maturation medium were maintained in the dark, at 25 ± 2 ºC for 40 days, until the formation of globular somatic embryo structures.

Calli from each cell line during the proliferation and PEMs containing somatic embryos at the maturation stage were collected and divided into three biological replicates. All samples collected were immediately frozen in liquid nitrogen and stored at -80ºC until further use. The samples were codified as Responsive cell line during proliferation (RP) and maturation (RM) stage, respectively; and similarly for Blocked cell line in proliferation (BP) and maturation (BM).

Rna Extraction And Processing

Total RNA was isolated using the ReliaPrep™ RNA Cell Miniprep System kit (Promega), according to the manufacturer's instructions for isolation of RNA from non-fibrous tissue and with minor modifications: (i) Polyvinypolypyrrolidone 10% (w/w) was added to each 100 mg FW samples; and (ii) when the lysate was transferred to a minicolumn, the centrifugation, when required, was performed twice to assure the maximum recovery of samples from the minicolumn. This method allowed the extract of both small (< 200 nt) and large (> 200 nt) RNA. Quantification and quality of RNA samples were double-checked by 1% agarose gel electrophoresis, as well as with the nano Agilent 2100 Bioanalyzer. The RNA Integrity Number (RIN) for the RNA isolated ranged from 6.6 to 8.4 for all samples. The same set of RNA samples was used for RT-qPCR validation.

Small Rna Library Construction And Sequencing

Twelve sRNA libraries (RP, RM, BP, and BM; $n = 3$) were produced using the TruSeq Small RNA Library Prep (Illumina), according to the manufacturer's instructions. Briefly, library construction followed the successive steps: (i) ligation of the 3' and 5' RNA adapters; (ii) reverse transcription, amplification, and quantification of libraries; (iii) purification of the cDNA construct; and (iv) checking of size, purity, and integrity of libraries. High-throughput sequencing was performed with Illumina Hiseq 2500 using single-end reads of 36 bp, in two lanes, with the Illumina TruSeq Rapid SBS Kit.

Bioinformatic Analysis Of Srnas

The sequencing data processing and sRNAs analysis pipeline is illustrated in Fig. 2. The data output from Illumina was processed and manipulated through Galaxy platform version 22.01 (Afgan et al. 2018) in a local server. Small RNA reads were trimmed to remove adapters using Trim Galore! (https://github.com/FelixKrueger/TrimGalore). Reads of 18–25 nt were filtered using Cutadapt (Martin 2011). Quality visualization was performed using FastQC and reads with quality above PHRED score 30 were selected (Andrews 2019).

Ribosome- (rRNA), transfer- (tRNA), small nuclear- (snRNA), small nucleolar- (snoRNA), transfer-messenger- (tmRNA), small conditional – (scRNA), trans-acting small interfering RNA- (tasiRNA), and other sRNAs, obtained from RNAcentral (The RNAcentral Consortium 2019) were identified through alignment using Bowtie (Langmead et al. 2009) and removed from the dataset. Unmapped reads were considered potential miRNAs for further analysis.

Mirnas Identification And Annotation

miRDeep2 (Friedländer et al. 2012) was used for the identification of conserved and novel miRNAs, as well as the prediction of miRNA precursor sequences. Firstly, conserved mature miRNAs were identified based on conserved miRNA sequences from Viridiplantae reported in miRbase release 22.1 (Kozomara et al. 2019) as input to map against *A. angustifolia* clean sRNAs, allowing no mismatches. The unmapped reads were considered candidates for novel miRNAs analysis.

Both annotated and non-annotated sRNA sequences were processed to identify putative novel miRNAs and precursor sequences for all miRNAs identified. The sRNA sequences were aligned to the *A. angustifolia* transcriptome (Elbl et al. 2015a), which evaluated differences in early somatic and zygotic embryogenesis and seed development.

In each alignment, a potential precursor sequence of 250 nt in length was excised and its secondary structure and minimum free energy were determined with the miRDeep2 package. Mature miRNAs were predicted based on the compatibility of the small RNA with the structure of its precursor. When both 5p and 3p miRNA reads were detected, the most abundant strand was labeled as the mature miRNA and the less abundant strand as the star sequence.

Differential Expression Analysis

miRNAs with counts of less than 10 in each group of replicates were removed. The expression values of miRNAs were normalized by counts per million (CPM). Differential accumulation analyses were performed following the standard protocol from the Bioconductor package EdgeR (Robinson et al. 2010). A pairwise comparison was conducted to detect the miRNAs with significant expression

differences between BP-RP, BM-RM, RM-RP, and BM-BP groups, considering FDR < 0.01 (*P*-adj < 0.01) and Log_2FC. All graphs were developed from Galaxy' outputs and using the R packages gplot, ggplot2, and Heatmap2.

Prediction And Functional Analysis Of Mirna Targets

Putative targets were identified using the psRNATarget online tool (Plant Small RNA Target Analysis Server) (Dai et al. 2018; https://www.zhaolab.org/psRNATarget/), using the V2 Schema with default configurations. This tool predicts the target genes based on reverse complementary matching. A 2.5 expectation value was used as a cut-off. The *A. angustifolia* transcriptome (Elbl et al. 2015a) was used as the target database.

To assess the predicted localization, molecular function, and involvement in biological processes of each miRNA target, functional annotation of the unique targets was performed with Trinotate v.3.2.1 pipeline (http://trinotate.github.io). Initially, all transcripts were scanned with Transdecoder v.5.5.0 (http://transdecoder.github.io) for extraction of long ORFs. Then, a homology search was included as retention criteria for coding region prediction. Functional domains were identified using Pfam v.33.1 domain database. Options '--retain_[pfam|blastp]_hits' were used to decrease false positives on ORF detection, and '--single_best_only' to recover the longest ORF. A combination of rules was applied to find the best single hit, including e-value < 1e-5 and coverage > 80%. Annotation was then followed by mapping to UniProtKB/Swiss-Prot 2020_04 database. Results from this analysis were loaded into an SQLite local database using the Trinotate tool. Transcripts were also functionally annotated based on Gene Ontology (GO) terms (v.2020-04, Trinotate), characterized according to the cellular component, the molecular function, and the biological process.

Stem-loop Rt And Rt-qpcr For Mirnas And Their Respective Targets

The Stem-loop RT method was employed according to Varkonyi-Gasic et al. (2007) with modifications. Reverse transcription was performed using SuperScript® IV First-Strand Synthesis System (ThermoFischer Scientific®), combining 500 ng of total DNA-free RNA (treated with DNAse I) with 10 ng random primers and 2 µM stem-loop primer, final concentration. Specific stem-loop primers were designed according to Varkonyi-Gasic et al. (2007) (Supplementary Table S7).

For RT-qPCR assay, gene- and miRNA-specific primers were designed using the OligoAnalyzer online tool (http://www.idtdna.com/calc/analyzer) according to the Minimum Information for Publication of RT-qPCR Experiments (MIQE) guidelines (Bustin et al. 2009). Quantification cycle (Cq) values from two technical replicates and primer efficiency were calculated using the linRegPCR software (Ruijter et al. 2009). Before the expression analysis, the set of reference genes described by Elbl et al. (2015b) was analyzed and checked for our experimental design. Gene expression values were normalized against geometric averages of the *AaEF-1α* (elongation factor 1α) and *AaEIF4B-L* (translational initiation factor 4B) reference genes (Elbl et al. 2015b). Calculations of gene relative expression were based on average expression levels, according to pairwise comparison. A gene was considered inhibited by its corresponding miRNA when its expression values showed opposite profiles.

Statistical analysis

RT-qPCR gene expression data were analyzed by analysis of variance (ANOVA), followed by Student's *t* or Tukey's test and log-transformed when appropriate. Statistical analyses were performed with 'R' (version 3.2.2, http://cran.r-project.org/).

Results

Overview of the A. angustifolia somatic embryogenesis small RNA transcriptome

To obtain a comprehensive sRNA transcriptome of the *A. angustifolia* somatic embryogenesis, we constructed 12 sRNA libraries of two cell lines with contrasting embryogenic potential [Responsive (R) or Blocked (B) to agents of maturation] during proliferation (P) and maturation (M) stages (RP, BP, RM, BM; $n = 3$) (Fig. 1). For each library, sRNAs were collected, pooled together, and sequenced using Illumina high-throughput technology. A flowchart of the sRNA analysis pipeline is available in Fig. 2. The full sequencing dataset will be available through Sequence Read Archive (SRA) at NCBI under identification number (*will be deposited at an appropriate time*).

We obtained between 22M and 44M raw reads per library and almost 400M raw reads in total (Suppl. Table S1). Clean small RNA reads were acquired from each library after removing adapters and low-quality reads when appropriated, as well as reads longer than

25-nt and shorter than 18-nt. Clean libraries constituted ~ 140M reads (36% of the total raw reads) (Suppl. Table S1). Reads were filtered to remove non-miRNAs and all matched sRNA sequences were categorized into putative sRNA classes (e.g., snRNA, snoRNA, tRNA, tmRNA, scRNA, tasiRNA and other sRNAs). Unmatched reads (44.62%) (Table 1) were used to identify conserved and novel miRNAs in *A. angustifolia*. Most non-miRNAs-reads were rRNA (50%). After cleanup and filtering, we obtained an average of 4.5M, 40M, 2.5M, and 16M reads in the RP, RM, BP, and BM libraries, respectively (Table 1). The percentages and counts of filtered reads were consistent among biological replicates (Suppl. Table S2).

The read size distribution revealed that the majority of filtered sRNAs are 21-nt, 23-nt, and 24-nt (Suppl. Figure 1). The 24-nt reads are highly expressed, accounting for 40% of the total number of reads, followed by 21-nt (16%) and 23-nt (14%). About 50% of 21-nt filtered sRNAs mostly started with 'U' as the first base, while 23–25-nt filtered sRNAs mostly started proportionally with 'A' and 'U' (30–44%) (Fig. 3A, B). Besides, we found that about 45.5% of the total filtered sRNAs also had a clear preference for cytosine (23-nt) and uridine (24-nt) as the last nucleotide (Suppl. Fig. S2).

Identification of conserved and novel miRNAs in A. angustifolia somatic embryogenesis

To identify conserved and novel miRNAs, unmatched sRNAs obtained during the filtering step were used. As the *A. angustifolia* genome is not available, known plant miRNAs (Viridiplantae) were downloaded from the miRbase 22.1 (www.mirbase.org) (Kozomara et al. 2019) and used as a reference for conserved miRNA mapping. Unannotated sRNAs were used to predict novel miRNAs and potential miRNA seeds. Those annotated as mature miRNA sequences were aligned to the *A. angustifolia* transcriptome (Elbl et al. 2015a) to identify likely miRNA precursors. For each alignment obtained, a flanking region of mRNA was extracted and its secondary structure was predicted through the miRDeep2 program (Friedländer et al. 2012). This analysis led to the prediction and identification of 165 miRNAs in 12 libraries of *A. angustifolia* somatic embryogenesis, classified into 143 novel and 22 conserved plant miRNAs (Suppl. Tables S3 and S4) distributed in 7 families (Suppl. Fig. S3).

The conserved miRNAs identified in *A. angustifolia*, such as miR156, miR169, miR394, miR482, miR536, miR1030, and miR1314 showed high sequence similarity to their homologs in Viridiplantae, including in *Glycine max, Malus domestica, Manihot esculenta, Oryza sativa, Picea abies, Physcomitrella patens, Sorghum bicolor, Vitis vinifera*, and *Zea mays* (Fig. 4A). The secondary structure of precursors was determined (Fig. 4B) based on identified precursor sequence (Suppl. File E1). We found 77 miRNAs sequences anchored in the 5p-arm and 88 miRNAs anchored in the 3p-arm (Suppl. Tables S3 and S4; Suppl. Files F1 and F2).

The overall distribution of miRNAs among group samples is represented by a Venn diagram (Fig. 4C). A total of 130 miRNAs were found to be shared among all libraries. The remaining miRNAs were assigned to be shared among two or more groups. Only one miRNA (Aang-miR169a) was exclusive to the group sample RM (Fig. 4C). Specific shared miRNAs pairwise comparison is available in Suppl. Fig. S4. Comparing the responsiveness factor, 130 miRNAs were shared between RP and BP samples, whereas 12 miRNAs were exclusive to the RP group and 4 miRNAs to BP (Fig. 4C, Suppl. Fig. S4A). During the maturation stage, 163 miRNAs were common between the cell lines, and only 1 miRNA was found exclusive to each group (Fig. 4C, Suppl. Fig. S4B). In the transition from proliferation to maturation, 142 miRNAs were shared between the two stages of the responsive cell line (RP-RM), while 22 miRNAs were exclusively found during the maturation stage (RM) (Fig. 4C, Suppl. Fig. S4C). For the blocked cell line, 134 miRNAs were found in both stages (BP and BM), and 30 miRNAs were exclusive to the maturation (BM) (Fig. 4C, Suppl Fig. S4D). The list of exclusive and common miRNAs is available in Suppl. Excel File E2.

Differentially Expressed Mirnas During Somatic Embryogenesis

To investigate whether the identified miRNAs are differentially expressed between the two contrasting cell lines of *A. angustifolia*, and during the transition from proliferation to maturation, we profiled a differential expression analysis using the EdgeR package. For this, miRNA expression levels were compared in four different ways: RP–BP, RM–BM, RM–RP, and BM–BP (Fig. 5). All the conserved and novel mature miRNAs with > 10 reads in each library were analyzed. Ninety differentially expressed miRNAs (P-value < 0.01, FDR < 0.01) that exhibited LogFC > 1.5 were selected between each pairwise comparison (Table 2). More up- than down-regulated miRNAs were found among the four pairwise comparisons (Fig. 5). The highest numbers of differentially up- and down-regulated miRNAs were found during the transition from proliferation to maturation in both cell lines (RP-RM and BP-BM), followed by a comparison between cell lines in proliferation and maturation separately (RP-BP and RM-BM) (Fig. 5).

Table 2
Differentially expressed miRNAs in *Araucaria angustifolia* cell lines with different embryogenic potential, during cell proliferation and maturation stages.

miRNA	RP/BP[a]			RM/BM[a]			RM/RP[a]			BM/BP[a]		
	LogFC[b]	*p*-value[b]	FDR[b]	LogFC[b]	*p*-value[b]	FDR[b]	LogFC[b]	*p*-value[b]	FDR[b]	LogFC[b]	*p*-value[b]	FDR[b]
Aang-miR156a	0.148	8.60E-01	9.30E-01	-1.230	2.09E-03	5.84E-03	0.698	3.11E-01	3.58E-01	1.698	1.44E-02	2.1E-02
Aang-miR394a	NA	NA	NA	NA	NA	NA	NA	NA	NA	-0.524	4.68E-01	5.5E-01
Aang-miR482a	-0.711	2.08E-08	2.21E-07	-0.647	5.82E-05	3.99E-04	0.377	3.96E-02	5.37E-02	-0.095	6.62E-01	7.1E-01
Aang-miR482b	-0.711	2.08E-08	2.21E-07	-0.647	5.82E-05	3.99E-04	0.377	3.96E-02	5.37E-02	-0.095	6.62E-01	7.1E-01
Aang-miR482c	-0.711	2.08E-08	2.21E-07	-0.647	5.82E-05	3.99E-04	0.377	3.96E-02	5.37E-02	-0.095	6.62E-01	7.1E-01
Aang-miR482d	-0.711	2.08E-08	2.21E-07	-0.647	5.82E-05	3.99E-04	0.377	3.96E-02	5.37E-02	-0.095	6.62E-01	7.1E-01
Aang-miR482e	0.562	3.83E-02	8.28E-02	0.537	2.79E-03	7.06E-03	0.427	8.73E-02	1.12E-01	0.091	7.22E-01	7.5E-01
Aang-miR482f	0.562	3.83E-02	8.28E-02	0.537	2.79E-03	7.06E-03	0.427	8.73E-02	1.12E-01	0.091	7.22E-01	7.5E-01
Aang-miR482g	0.562	3.83E-02	8.28E-02	0.537	2.79E-03	7.06E-03	0.427	8.73E-02	1.12E-01	0.091	7.22E-01	7.5E-01
Aang-miR482h	-0.404	7.74E-02	1.44E-01	-1.461	1.99E-06	3.51E-05	-1.262	1.88E-05	4.02E-05	-0.622	1.06E-02	1.6E-02
Aang-miR482i	-0.404	7.74E-02	1.44E-01	-1.461	1.99E-06	3.51E-05	-1.262	1.88E-05	4.02E-05	-0.622	1.06E-02	1.6E-02
Aang-miR482j	-0.084	5.45E-01	7.72E-01	-0.384	1.00E-01	1.47E-01	**-2.878**	**1.56E-14**	**2.38E-13**	**-2.987**	**8.22E-34**	**3.4E-32**
Aang-miR536a	NA	NA	NA	0.982	5.55E-02	9.62E-02	**6.796**	**9.93E-04**	**1.77E-03**	NA	NA	NA
Aang-miR536b	NA	NA	NA	0.982	5.55E-02	9.62E-02	**6.796**	**9.93E-04**	**1.77E-03**	NA	NA	NA
Aang-miR536c	NA	NA	NA	0.982	5.55E-02	9.62E-02	**6.796**	**9.93E-04**	**1.77E-03**	NA	NA	NA
Aang-miR536d	NA	NA	NA	0.982	5.55E-02	9.62E-02	**6.796**	**9.93E-04**	**1.77E-03**	NA	NA	NA
Aang-miR536e	NA	NA	NA	0.982	5.55E-02	9.62E-02	**6.796**	**9.93E-04**	**1.77E-03**	NA	NA	NA
Aang-miR1030a	0.187	7.82E-01	9.30E-01	-1.189	6.72E-05	4.20E-04	**2.158**	**3.29E-05**	**6.94E-05**	**3.139**	**3.74E-11**	**1.7E-10**
Aang-miR1314a	0.221	5.25E-01	7.72E-01	0.354	8.66E-02	1.29E-01	**2.667**	**5.15E-11**	**3.21E-10**	**2.152**	**6.45E-11**	**2.6E-10**
Aang-miR1314b	0.221	5.25E-01	7.72E-01	0.354	8.66E-02	1.29E-01	**2.667**	**5.15E-11**	**3.21E-10**	**2.152**	**6.45E-11**	**2.6E-10**

[a] RP, responsive cell line during proliferation stage; BP, blocked cell line during proliferation stage; RM, responsive during maturation stage; and BM, blocked during the maturation stage.

[b] Bold values indicate LogFC > 1.5, *P*-value < 0.01, and FDR < 0.01.

miRNA	RP/BP[a]			RM/BM[a]			RM/RP[a]			BM/BP[a]		
	LogFC[b]	*p*-value[b]	FDR[b]	LogFC[b]	*p*-value[b]	FDR[b]	LogFC[b]	*p*-value[b]	FDR[b]	LogFC[b]	*p*-value[b]	FDR[b]
Aang-miR1314c	0.221	5.25E-01	7.72E-01	0.354	8.66E-02	1.29E-01	**2.667**	**5.15E-11**	**3.21E-10**	**2.152**	**6.45E-11**	**2.6E-10**
Aang-novel_1	0.383	2.41E-04	1.22E-03	-1.125	9.04E-06	9.52E-05	-1.202	1.02E-07	3.11E-07	-0.102	6.41E-01	7.1E-01
Aang-novel_2	0.383	2.41E-04	1.22E-03	-1.125	9.04E-06	9.52E-05	-1.202	1.02E-07	3.11E-07	-0.102	6.41E-01	7.1E-01
Aang-novel_3	-0.758	9.77E-06	5.45E-05	-0.678	2.63E-03	7.06E-03	-1.303	1.03E-08	4.41E-08	**-1.820**	**7.68E-15**	**4.5E-14**
Aang-novel_4	0.901	3.58E-09	9.49E-08	0.402	1.29E-01	1.79E-01	**2.226**	**6.82E-13**	**8.49E-12**	**2.317**	**1.40E-23**	**1.1E-22**
Aang-novel_5	-0.028	7.79E-01	9.30E-01	-0.057	5.34E-01	5.95E-01	1.471	4.14E-10	2.10E-09	1.099	2.44E-07	7.5E-07
Aang-novel_6	-0.028	7.79E-01	9.30E-01	-0.057	5.34E-01	5.95E-01	1.471	4.14E-10	2.10E-09	1.099	2.44E-07	7.5E-07
Aang-novel_7	0.245	5.29E-03	1.52E-02	-0.542	8.15E-03	1.86E-02	**-2.852**	**9.23E-18**	**1.58E-16**	**-2.458**	**6.85E-25**	**6.5E-24**
Aang-novel_8	0.245	5.29E-03	1.52E-02	-0.542	8.15E-03	1.86E-02	**-2.852**	**9.23E-18**	**1.58E-16**	**-2.458**	**6.85E-25**	**6.5E-24**
Aang-novel_9	-0.001	9.91E-01	9.91E-01	1.136	7.70E-05	4.20E-04	0.029	8.70E-01	8.70E-01	**-1.522**	**1.27E-12**	**6.3E-12**
Aang-novel_10	0.217	3.34E-02	7.69E-02	-0.170	1.24E-01	1.73E-01	-0.467	1.22E-02	1.83E-02	-0.472	2.12E-02	3.1E-02
Aang-novel_11	0.029	8.17E-01	9.30E-01	-0.466	4.83E-02	8.94E-02	**1.884**	**1.25E-11**	**1.01E-10**	**1.965**	**5.49E-20**	**4.0E-19**
Aang-novel_12	-0.009	9.11E-01	9.30E-01	-0.877	5.55E-04	1.95E-03	**-3.042**	**9.09E-19**	**2.49E-17**	**-2.559**	**5.34E-28**	**9.4E-27**
Aang-novel_13	-0.009	9.11E-01	9.30E-01	-0.877	5.55E-04	1.95E-03	**-3.042**	**9.09E-19**	**2.49E-17**	**-2.559**	**5.34E-28**	**9.4E-27**
Aang-novel_14	-0.009	9.11E-01	9.30E-01	-0.877	5.55E-04	1.95E-03	**-3.042**	**9.09E-19**	**2.49E-17**	**-2.559**	**5.34E-28**	**9.4E-27**
Aang-novel_15	-0.009	9.11E-01	9.30E-01	-0.877	5.55E-04	1.95E-03	**-3.042**	**9.09E-19**	**2.49E-17**	**-2.559**	**5.34E-28**	**9.4E-27**
Aang-novel_16	0.242	2.27E-02	6.20E-02	-1.413	1.21E-05	1.18E-04	-0.936	1.34E-05	2.96E-05	0.329	9.59E-02	1.3E-01
Aang-novel_17	-0.350	3.46E-03	1.08E-02	0.044	7.47E-01	7.93E-01	0.559	4.68E-03	7.29E-03	-0.239	2.22E-01	2.9E-01
Aang-novel_18	0.655	4.56E-06	2.69E-05	0.548	6.92E-04	2.12E-03	0.137	4.61E-01	4.93E-01	-0.146	4.54E-01	5.4E-01
Aang-novel_19	-0.313	3.32E-02	7.69E-02	0.055	7.06E-01	7.55E-01	**1.851**	**5.91E-12**	**5.40E-11**	1.087	5.51E-08	1.8E-07
Aang-novel_20	-0.313	3.32E-02	7.69E-02	0.055	7.06E-01	7.55E-01	**1.851**	**5.91E-12**	**5.40E-11**	1.087	5.51E-08	1.8E-07

[a] RP, responsive cell line during proliferation stage; BP, blocked cell line during proliferation stage; RM, responsive during maturation stage; and BM, blocked during the maturation stage.

[b] Bold values indicate LogFC > 1.5, *P*-value < 0.01, and FDR < 0.01.

miRNA	RP/BP[a]			RM/BM[a]			RM/RP[a]			BM/BP[a]		
	LogFC[b]	*p*-value[b]	FDR[b]	LogFC[b]	*p*-value[b]	FDR[b]	LogFC[b]	*p*-value[b]	FDR[b]	LogFC[b]	*p*-value[b]	FDR[b]
Aang-novel_21	-0.711	1.32E-03	4.75E-03	-0.662	4.02E-04	1.63E-03	**2.291**	**1.11E-13**	**1.52E-12**	**1.837**	**5.24E-18**	**3.4E-17**
Aang-novel_22	-0.953	7.74E-09	1.37E-07	-0.436	1.72E-02	3.57E-02	-1.242	3.41E-08	1.30E-07	**-2.164**	**2.24E-24**	**1.8E-23**
Aang-novel_23	-0.953	7.74E-09	1.37E-07	-0.436	1.72E-02	3.57E-02	-1.242	3.41E-08	1.30E-07	**-2.164**	**2.24E-24**	**1.8E-23**
Aang-novel_24	-1.119	4.41E-08	3.89E-07	0.349	1.56E-01	2.04E-01	0.842	1.20E-03	2.02E-03	-0.996	2.65E-07	7.7E-07
Aang-novel_25	-1.119	4.41E-08	3.89E-07	0.349	1.56E-01	2.04E-01	0.842	1.20E-03	2.02E-03	-0.996	2.65E-07	7.7E-07
Aang-novel_26	-0.061	6.47E-01	8.89E-01	0.016	9.08E-01	9.15E-01	**-1.770**	**7.00E-11**	**4.00E-10**	**-2.243**	**7.01E-27**	**9.6E-26**
Aang-novel_27	-0.061	6.47E-01	8.89E-01	0.016	9.08E-01	9.15E-01	**-1.770**	**7.00E-11**	**4.00E-10**	**-2.243**	**7.01E-27**	**9.6E-26**
Aang-novel_28	-0.550	4.40E-03	1.33E-02	0.256	7.78E-02	1.20E-01	1.145	8.75E-06	2.00E-05	-0.049	8.12E-01	8.1E-01
Aang-novel_29	-1.015	8.95E-04	3.95E-03	-0.150	3.37E-01	4.09E-01	**2.156**	**1.45E-09**	**6.86E-09**	0.885	4.37E-04	9.9E-04
Aang-novel_30	-0.940	7.93E-08	6.01E-07	-1.036	6.95E-04	2.12E-03	**-2.317**	**1.71E-12**	**1.80E-11**	**-2.627**	**3.36E-34**	**2.1E-32**
Aang-novel_31	-0.062	8.27E-01	9.30E-01	0.120	3.57E-01	4.29E-01	1.013	5.15E-04	9.80E-04	0.463	7.90E-02	1.1E-01
Aang-novel_32	-1.089	1.79E-06	1.12E-05	-0.235	1.36E-01	1.84E-01	-0.420	1.08E-01	1.30E-01	**-1.669**	**1.93E-13**	**9.9E-13**
Aang-novel_33	-1.089	1.79E-06	1.12E-05	-0.235	1.36E-01	1.84E-01	-0.420	1.08E-01	1.30E-01	**-1.669**	**1.93E-13**	**9.9E-13**
Aang-novel_34	0.495	5.46E-01	7.72E-01	-0.088	8.25E-01	8.63E-01	**3.213**	**3.12E-07**	**9.30E-07**	**3.449**	**5.03E-10**	**1.9E-09**
Aang-novel_35	0.236	6.66E-01	8.93E-01	0.895	2.00E-02	3.98E-02	**2.448**	**2.73E-08**	**1.10E-07**	1.406	2.97E-03	5.1E-03
Aang-novel_36	-0.433	1.41E-01	2.53E-01	-0.028	8.90E-01	9.15E-01	-0.051	8.58E-01	8.65E-01	-0.882	5.22E-03	8.7E-03
Aang-novel_37	-0.797	7.77E-04	3.58E-03	-0.571	2.87E-02	5.46E-02	**-2.666**	**8.93E-12**	**7.64E-11**	**-3.268**	**4.71E-26**	**5.3E-25**
Aang-novel_38	-1.189	2.80E-01	4.86E-01	0.342	3.07E-01	3.76E-01	**4.058**	**1.56E-06**	**4.26E-06**	**2.066**	**9.14E-04**	**1.8E-03**
Aang-novel_39	-1.189	2.80E-01	4.86E-01	0.342	3.07E-01	3.76E-01	**4.058**	**1.56E-06**	**4.26E-06**	**2.066**	**9.14E-04**	**1.8E-03**
Aang-novel_40	-0.042	8.94E-01	9.30E-01	-0.764	7.58E-03	1.79E-02	-0.489	1.67E-01	1.97E-01	-0.174	6.19E-01	7.1E-01
Aang-novel_41	-0.042	8.94E-01	9.30E-01	-0.764	7.58E-03	1.79E-02	-0.489	1.67E-01	1.97E-01	-0.174	6.19E-01	7.1E-01

[a] RP, responsive cell line during proliferation stage; BP, blocked cell line during proliferation stage; RM, responsive during maturation stage; and BM, blocked during the maturation stage.

[b] Bold values indicate LogFC > 1.5, *P*-value < 0.01, and FDR < 0.01.

miRNA	RP/BP[a]			RM/BM[a]			RM/RP[a]			BM/BP[a]		
	LogFC[b]	*p*-value[b]	FDR[b]	LogFC[b]	*p*-value[b]	FDR[b]	LogFC[b]	*p*-value[b]	FDR[b]	LogFC[b]	*p*-value[b]	FDR[b]
Aang-novel_42	1.095	6.34E-08	5.17E-07	1.360	1.43E-06	3.51E-05	0.980	2.80E-06	6.61E-06	0.309	1.21E-01	1.6E-01
Aang-novel_43	-0.978	3.57E-01	5.83E-01	0.333	4.59E-01	5.24E-01	**3.852**	**1.68E-06**	**4.26E-06**	**2.102**	**1.48E-03**	**2.7E-03**
Aang-novel_44	-0.978	3.57E-01	5.83E-01	0.333	4.59E-01	5.24E-01	**3.852**	**1.68E-06**	**4.26E-06**	**2.102**	**1.48E-03**	**2.7E-03**
Aang-novel_45	-0.978	3.57E-01	5.83E-01	0.333	4.59E-01	5.24E-01	**3.852**	**1.68E-06**	**4.26E-06**	**2.102**	**1.48E-03**	**2.7E-03**
Aang-novel_46	NA	NA	NA	1.017	2.83E-03	7.06E-03	**4.357**	**7.28E-09**	**3.22E-08**	**4.421**	**1.55E-05**	**4.0E-05**
Aang-novel_47	-1.250	4.09E-04	1.97E-03	**-4.752**	**2.05E-06**	**3.51E-05**	**-5.194**	**4.67E-11**	**3.21E-10**	**-2.147**	**7.37E-09**	**2.7E-08**
Aang-novel_48	1.132	2.51E-03	8.31E-03	NA	NA	NA	**-4.094**	**2.34E-10**	**1.28E-09**	**-3.725**	**2.97E-11**	**1.4E-10**
Aang-novel_49	NA	NA	NA	-0.907	1.38E-01	1.85E-01	NA	NA	NA	0.706	3.19E-01	3.9E-01
Aang-novel_50	NA	NA	NA	-0.514	1.82E-01	2.35E-01	2.496	1.13E-02	1.73E-02	1.999	2.20E-02	3.2E-02
Aang-novel_51	NA	NA	NA	1.103	1.46E-02	3.12E-02	2.860	1.23E-02	1.84E-02	NA	NA	NA
Aang-novel_52	NA	NA	NA	-0.642	1.13E-01	1.60E-01	0.442	5.47E-01	5.77E-01	**6.628**	**8.28E-04**	**1.7E-03**
Aang-novel_53	NA	NA	NA	-0.642	1.13E-01	1.60E-01	0.442	5.47E-01	5.77E-01	**6.628**	**8.28E-04**	**1.7E-03**
Aang-novel_54	NA	NA	NA	-0.106	8.25E-01	8.63E-01	NA	NA	NA	NA	NA	NA
Aang-novel_58	-1.815	4.28E-02	8.73E-02	NA	NA	NA	NA	NA	NA	**-2.395**	**1.84E-04**	**4.4E-04**
Aang-novel_59	-1.815	4.28E-02	8.73E-02	NA	NA	NA	NA	NA	NA	**-2.395**	**1.84E-04**	**4.4E-04**
Aang-novel_60	-1.815	4.28E-02	8.73E-02	NA	NA	NA	NA	NA	NA	**-2.395**	**1.84E-04**	**4.4E-04**
Aang-novel_61	NA	NA	NA	0.084	8.99E-01	9.15E-01	NA	NA	NA	NA	NA	NA
Aang-novel_63	0.823	5.35E-01	7.72E-01	NA	NA	NA	-0.190	8.08E-01	8.20E-01	NA	NA	NA
Aang-novel_64	0.536	1.13E-01	2.07E-01	0.892	2.49E-02	4.81E-02	-1.488	4.70E-04	9.08E-04	**-2.256**	**7.13E-06**	**1.9E-05**
Aang-novel_66	NA	NA	NA	0.812	7.09E-02	1.12E-01	**6.150**	**2.51E-03**	**3.99E-03**	NA	NA	NA
Aang-novel_67	NA	NA	NA	0.812	7.09E-02	1.12E-01	**6.150**	**2.51E-03**	**3.99E-03**	NA	NA	NA

[a] RP, responsive cell line during proliferation stage; BP, blocked cell line during proliferation stage; RM, responsive during maturation stage; and BM, blocked during the maturation stage.

[b] Bold values indicate LogFC > 1.5, *P*-value < 0.01, and FDR < 0.01.

miRNA	RP/BP[a]			RM/BM[a]			RM/RP[a]			BM/BP[a]		
	LogFC[b]	*p*-value[b]	FDR[b]	LogFC[b]	*p*-value[b]	FDR[b]	LogFC[b]	*p*-value[b]	FDR[b]	LogFC[b]	*p*-value[b]	FDR[b]
Aang-novel_68	NA	NA	NA	0.812	7.09E-02	1.12E-01	**6.150**	**2.51E-03**	**3.99E-03**	NA	NA	NA
Aang-novel_69	NA	NA	NA	**1.640**	**2.78E-03**	**7.06E-03**	1.026	2.07E-01	2.41E-01	NA	NA	NA
Aang-novel_70	NA	NA	NA	**2.725**	**1.54E-03**	**4.40E-03**	2.672	2.31E-02	3.36E-02	NA	NA	NA
Aang-novel_71	NA	NA	NA	**2.285**	**2.82E-04**	**1.25E-03**	**6.580**	**1.06E-03**	**1.84E-03**	NA	NA	NA
Aang-novel_72	-0.175	6.78E-01	8.97E-01	-1.172	5.65E-03	1.38E-02	-1.166	2.95E-02	4.25E-02	-0.539	2.64E-01	3.4E-01
Aang-novel_73	NA	NA	NA	**2.285**	**2.82E-04**	**1.25E-03**	**6.580**	**1.06E-03**	**1.84E-03**	NA	NA	NA
Aang-novel_74	NA	NA	NA	1.489	4.71E-04	1.84E-03	**3.215**	**1.77E-04**	**3.57E-04**	2.813	1.28E-02	1.9E-02
Aang-novel_75	**-3.403**	**9.00E-19**	**4.77E-17**	**-2.329**	**2.91E-06**	**3.63E-05**	**-3.821**	**3.73E-18**	**8.51E-17**	**-5.310**	**2.79E-77**	**3.4E-75**
Aang-novel_77	NA	NA	NA	**3.026**	**1.34E-03**	**3.91E-03**	**6.081**	**2.84E-03**	**4.47E-03**	NA	NA	NA
Aang-novel_78	NA	NA	NA	**-3.367**	**1.26E-06**	**3.51E-05**	2.269	4.28E-02	5.64E-02	**3.655**	**4.31E-07**	**1.2E-06**
Aang-novel_79	NA	NA	NA	**-3.367**	**1.26E-06**	**3.51E-05**	2.269	4.28E-02	5.64E-02	**3.655**	**4.31E-07**	**1.2E-06**
Aang-novel_80	0.578	2.96E-03	9.52E-03	0.514	4.53E-02	8.50E-02	**-1.998**	**7.85E-10**	**3.84E-09**	**-2.344**	**9.29E-19**	**6.3E-18**
Aang-novel_81	NA	NA	NA	**-3.367**	**1.26E-06**	**3.51E-05**	2.269	4.28E-02	5.64E-02	**3.655**	**4.31E-07**	**1.2E-06**
Aang-novel_82	0.373	2.52E-02	6.20E-02	0.706	8.50E-05	4.20E-04	1.266	7.89E-08	2.51E-07	0.543	6.32E-03	9.8E-03
Aang-novel_83	0.373	2.52E-02	6.20E-02	0.706	8.50E-05	4.20E-04	1.266	7.89E-08	2.51E-07	0.543	6.32E-03	9.8E-03
Aang-novel_84	0.373	2.52E-02	6.20E-02	0.706	8.50E-05	4.20E-04	1.266	7.89E-08	2.51E-07	0.543	6.32E-03	9.8E-03
Aang-novel_85	0.373	2.52E-02	6.20E-02	0.706	8.50E-05	4.20E-04	1.266	7.89E-08	2.51E-07	0.543	6.32E-03	9.8E-03
Aang-novel_86	0.373	2.52E-02	6.20E-02	0.706	8.50E-05	4.20E-04	1.266	7.89E-08	2.51E-07	0.543	6.32E-03	9.8E-03
Aang-novel_87	0.013	9.80E-01	9.90E-01	1.286	2.93E-05	2.68E-04	**3.107**	**1.75E-11**	**1.33E-10**	1.428	2.42E-03	4.2E-03
Aang-novel_88	-0.331	4.47E-01	6.86E-01	0.043	9.15E-01	9.15E-01	**-1.718**	**1.83E-03**	**3.01E-03**	**-2.519**	**1.35E-06**	**3.6E-06**
Aang-novel_89	-0.107	7.76E-01	9.30E-01	1.039	6.85E-04	2.12E-03	1.416	3.90E-05	8.10E-05	-0.143	7.29E-01	7.5E-01

[a] RP, responsive cell line during proliferation stage; BP, blocked cell line during proliferation stage; RM, responsive during maturation stage; and BM, blocked during the maturation stage.

[b] Bold values indicate LogFC > 1.5, *P*-value < 0.01, and FDR < 0.01.

miRNA	RP/BP[a]			RM/BM[a]			RM/RP[a]			BM/BP[a]		
	LogFC[b]	*p*-value[b]	FDR[b]	LogFC[b]	*p*-value[b]	FDR[b]	LogFC[b]	*p*-value[b]	FDR[b]	LogFC[b]	*p*-value[b]	FDR[b]
Aang-novel_90	-0.599	6.63E-02	1.33E-01	-0.234	3.63E-01	4.32E-01	**2.550**	**2.36E-09**	**1.08E-08**	**1.840**	**1.84E-13**	**9.9E-13**
Aang-novel_91	-0.203	4.12E-01	6.42E-01	-0.061	6.61E-01	7.19E-01	0.228	3.93E-01	4.33E-01	-0.280	3.01E-01	3.7E-01
Aang-novel_92	-0.203	4.12E-01	6.42E-01	-0.061	6.61E-01	7.19E-01	0.228	3.93E-01	4.33E-01	-0.280	3.01E-01	3.7E-01
Aang-novel_94	NA	NA	NA	-0.462	2.29E-01	2.85E-01	1.447	9.72E-02	1.20E-01	2.010	3.59E-02	5.0E-02
Aang-novel_95	NA	NA	NA	-0.462	2.29E-01	2.85E-01	1.447	9.72E-02	1.20E-01	2.010	3.59E-02	5.0E-02
Aang-novel_96	NA	NA	NA	-0.462	2.29E-01	2.85E-01	1.447	9.72E-02	1.20E-01	2.010	3.59E-02	5.0E-02
Aang-novel_97	-0.203	4.12E-01	6.42E-01	-0.061	6.61E-01	7.19E-01	0.228	3.93E-01	4.33E-01	-0.280	3.01E-01	3.7E-01
Aang-novel_98	NA	NA	NA	0.782	7.41E-02	1.15E-01	2.408	3.25E-02	4.64E-02	NA	NA	NA
Aang-novel_99	NA	NA	NA	**-6.759**	**1.04E-06**	**3.51E-05**	NA	NA	NA	**4.714**	**1.72E-10**	**6.8E-10**
Aang-novel_104	-0.978	3.57E-01	5.83E-01	0.333	4.59E-01	5.24E-01	**3.852**	**1.68E-06**	**4.26E-06**	**2.102**	**1.48E-03**	**2.7E-03**
Aang-novel_105	**1.552**	**9.08E-11**	**3.21E-09**	**1.813**	**2.89E-06**	**3.63E-05**	-1.483	1.09E-08	4.53E-08	**-2.112**	**1.50E-15**	**9.2E-15**
Aang-novel_106	0.080	9.12E-01	9.30E-01	1.310	1.24E-02	2.69E-02	**2.803**	**1.71E-06**	**4.26E-06**	1.186	5.67E-02	7.7E-02
Aang-novel_107	0.228	6.94E-01	8.97E-01	NA	NA	NA	**-3.168**	**2.12E-06**	**5.09E-06**	**-3.640**	**2.56E-08**	**8.7E-08**
Aang-novel_108	0.080	9.12E-01	9.30E-01	1.310	1.24E-02	2.69E-02	**2.803**	**1.71E-06**	**4.26E-06**	1.186	5.67E-02	7.7E-02
Aang-novel_109	0.228	6.94E-01	8.97E-01	NA	NA	NA	**-3.168**	**2.12E-06**	**5.09E-06**	**-3.640**	**2.56E-08**	**8.7E-08**
Aang-novel_110	NA	NA	NA	-0.337	5.33E-01	5.95E-01	NA	NA	NA	0.336	6.74E-01	7.2E-01
Aang-novel_112	**2.901**	**6.96E-07**	**4.92E-06**	**2.077**	**2.68E-06**	**3.63E-05**	1.357	1.01E-05	2.26E-05	**1.823**	**1.59E-03**	**2.8E-03**
Aang-novel_114	NA	NA	NA	NA	NA	NA	1.336	1.72E-01	2.01E-01	NA	NA	NA
Aang-novel_115	NA	NA	NA	**5.011**	**8.59E-05**	**4.20E-04**	2.694	1.93E-02	2.85E-02	NA	NA	NA
Aang-novel_116	0.238	8.40E-01	9.30E-01	**1.808**	**6.48E-04**	**2.11E-03**	**2.614**	**2.67E-04**	**5.23E-04**	0.700	3.82E-01	4.6E-01
Aang-novel_117	NA	NA	NA	**2.176**	**6.05E-04**	**2.07E-03**	1.878	9.34E-02	1.18E-01	NA	NA	NA

[a] RP, responsive cell line during proliferation stage; BP, blocked cell line during proliferation stage; RM, responsive during maturation stage; and BM, blocked during the maturation stage.

[b] Bold values indicate LogFC > 1.5, *P*-value < 0.01, and FDR < 0.01.

miRNA	RP/BP[a]			RM/BM[a]			RM/RP[a]			BM/BP[a]		
	LogFC[b]	*p*-value[b]	FDR[b]	LogFC[b]	*p*-value[b]	FDR[b]	LogFC[b]	*p*-value[b]	FDR[b]	LogFC[b]	*p*-value[b]	FDR[b]
Aang-novel_118	0.480	6.54E-01	8.89E-01	-0.482	2.11E-01	2.70E-01	-0.246	7.37E-01	7.59E-01	0.365	6.49E-01	7.1E-01
Aang-novel_119	0.101	7.33E-01	9.25E-01	1.440	4.50E-05	3.85E-04	0.794	6.89E-03	1.06E-02	-0.953	1.40E-02	2.1E-02
Aang-novel_120	**3.907**	**2.69E-19**	**2.85E-17**	-0.287	3.75E-01	4.43E-01	**-8.065**	**2.81E-31**	**3.84E-29**	**-4.269**	**2.76E-26**	**3.4E-25**
Aang-novel_121	0.238	8.40E-01	9.30E-01	**1.808**	**6.48E-04**	**2.11E-03**	**2.614**	**2.67E-04**	**5.23E-04**	0.700	3.82E-01	4.6E-01
Aang-novel_122	1.029	7.45E-02	1.44E-01	0.706	2.00E-02	3.98E-02	0.216	6.27E-01	6.50E-01	0.190	7.56E-01	7.6E-01
Aang-novel_123	0.080	7.29E-01	9.25E-01	0.437	8.45E-03	1.90E-02	0.857	1.65E-03	2.76E-03	0.111	6.82E-01	7.2E-01
Aang-novel_124	1.029	7.45E-02	1.44E-01	0.706	2.00E-02	3.98E-02	0.216	6.27E-01	6.50E-01	0.190	7.56E-01	7.6E-01
Aang-novel_126	NA	NA	NA	**2.430**	**4.03E-04**	**1.63E-03**	1.594	3.64E-02	5.14E-02	NA	NA	NA
Aang-novel_131	NA	NA	NA	**1.568**	**4.04E-04**	**1.63E-03**	**3.107**	**5.40E-06**	**1.25E-05**	**3.338**	**3.14E-03**	**5.3E-03**
Aang-novel_132	0.185	8.41E-01	9.30E-01	**2.334**	**8.94E-05**	**4.22E-04**	**3.153**	**9.32E-07**	**2.72E-06**	0.650	3.92E-01	4.7E-01
Aang-novel_133	-0.066	9.04E-01	9.30E-01	0.445	1.03E-01	1.48E-01	**2.432**	**5.91E-08**	**2.13E-07**	**1.527**	**4.23E-04**	**9.8E-04**
Aang-novel_134	NA	NA	NA	0.882	1.54E-01	2.04E-01	1.235	1.43E-01	1.72E-01	**6.153**	**2.46E-03**	**4.3E-03**
Aang-novel_135	-0.066	9.04E-01	9.30E-01	0.445	1.03E-01	1.48E-01	**2.432**	**5.91E-08**	**2.13E-07**	**1.527**	**4.23E-04**	**9.8E-04**
Aang-novel_136	1.007	2.36E-03	8.07E-03	0.055	8.50E-01	8.82E-01	**-3.156**	**9.61E-13**	**1.10E-11**	**-2.608**	**1.29E-09**	**4.8E-09**
Aang-novel_137	NA	NA	NA	**1.506**	**7.66E-04**	**2.28E-03**	**3.719**	**5.50E-05**	**1.12E-04**	**6.473**	**1.20E-03**	**2.3E-03**
Aang-novel_138	**2.687**	**1.35E-03**	**4.75E-03**	-0.525	6.99E-02	1.12E-01	-0.399	4.01E-01	4.33E-01	**2.533**	**6.71E-04**	**1.4E-03**
Aang-novel_139	**2.687**	**1.35E-03**	**4.75E-03**	-0.525	6.99E-02	1.12E-01	-0.399	4.01E-01	4.33E-01	**2.533**	**6.71E-04**	**1.4E-03**
Aang-novel_140	**2.687**	**1.35E-03**	**4.75E-03**	-0.525	6.99E-02	1.12E-01	-0.399	4.01E-01	4.33E-01	**2.533**	**6.71E-04**	**1.4E-03**
Aang-novel_141	**2.687**	**1.35E-03**	**4.75E-03**	-0.525	6.99E-02	1.12E-01	-0.399	4.01E-01	4.33E-01	**2.533**	**6.71E-04**	**1.4E-03**
Aang-novel_142	**2.687**	**1.35E-03**	**4.75E-03**	-0.525	6.99E-02	1.12E-01	-0.399	4.01E-01	4.33E-01	**2.533**	**6.71E-04**	**1.4E-03**
Aang-novel_143	NA	NA	NA	1.130	2.17E-02	4.24E-02	0.205	7.80E-01	7.97E-01	NA	NA	NA

[a] RP, responsive cell line during proliferation stage; BP, blocked cell line during proliferation stage; RM, responsive during maturation stage; and BM, blocked during the maturation stage.

[b] Bold values indicate LogFC > 1.5, *P*-value < 0.01, and FDR < 0.01.

A heatmap with the normalized read counts for all differentiated expressed (FDR < 0.01; *P*-value < 0.01; LogFC > 1.5) miRNAs identified for each pairwise comparison is shown in Figs. 6–8. The replicates of each sample group were clustered together, indicating that the results were consistent. In general, two clusters (CI and CII) of differentiated expressed miRNAs were observed for each pairwise comparison. A total of nine miRNAs showed differential expression between the RP and BP sample groups, eight were significantly up-regulated and only one (Aang-novel_75) was down-regulated in RP compared to BP (Table 2 and Fig. 6A). Among the conserved miRNAs identified, members from four miRNA families (miR156, miR482, miR1030, and miR1314) were differentially expressed (Table 2), but no one showed LogFC > 1.5 between RP and BP (Fig. 6A).

During the maturation stage, 21 miRNAs were differentially expressed between RM and BM cell lines, of which 15 were up-regulated in RM (CI) and six were up-regulated in BM (CII) (Fig. 6B). All these differentially expressed miRNAs (FDR < 0.01; *P* < 0.01; LogFC > 1.5) were identified as novel. Similar to the previous comparison, the largest number of up-regulated miRNAs are present in the responsive cell line.

The transition from proliferation to maturation stage in the two cell lines tested was also investigated. Sixty-two miRNAs were differentially expressed between RP and RM, representing about 45% of the total of miRNAs (137) expressed in these two libraries (Fig. 7). Among them, 42 and 20 miRNAs were up-regulated in RM (CI) and in RP (CII), respectively. Ten differentially expressed miRNAs between RM and RP are from four conserved families (miR482, miR536, miR1030, and miR1314). From these, nine miRNAs were up-regulated during the maturation stage, and Aang-miR482j was down-regulated (Fig. 7). Interestingly, five isoforms from the miR536 family were expressed almost 7-fold higher in RM when compared to RP (Table 2).

During the transition from proliferation to maturation, 64 from a total of 123 miRNAs were differentially expressed in the Blocked cell line (Table 2). Thirty-three miRNAs were up-regulated (CI) and 31 were down-regulated (CII) in BM compared to BP (Fig. 8). Five miRNAs from three conserved families (miR482, miR1030, and miR1314) were found. Aang-miR482j was 3-fold down-regulated in BM. In contrast to that observed in the Responsive cell line, in which the majority of the differentially expressed miRNAs was up-regulated during the maturation, miRNAs were similarly up- and down-regulated in the Blocked cell line.

Ninety-one differentially expressed miRNAs (conserved + novel) were exclusive or shared among the four pairwise comparison groups (Suppl. Fig. S5 and Suppl. File E3). Only miRNA Aang-novel_75 was shared among the four comparisons. Most of the differentially expressed miRNAs were shown to be condition-specific by the pairwise comparison. Five miRNAs were exclusive to the RM/BM comparison, 16 to RM/RP, and 13 to BM/BP. No exclusive differentially expressed miRNA was found in the RP/BP comparison. The remained differentially expressed miRNAs were shared among the four pairwise comparisons, 40 miRNAs were common to the transition from proliferation to maturation in both cell lines (RM/RP and BM/BP) and three common to the cell line genotypes (RP/BP and RM/BM).

Mirna Function And Gene Enrichment Analysis Of Predicted Mirna Targets

Target mRNAs of 22 conserved and 143 novel miRNAs were predicted based on the complementarity by using the web tool psRNATarget (Dai et al. 2018). Target annotations were obtained from our previous *A. angustifolia* transcriptome (Elbl et al. 2015a). A total of 98 potential target genes were found for 89 miRNAs (Figs. 9 and 10; Suppl. Table S5 and S6). Among these, 10 are targets of five conserved miRNAs, and 88 are targets of 84 novel miRNAs. Predicted targets were identified for the most novel miRNAs (84/143), whereas only a few were obtained for conserved miRNAs (5/22). Some conserved miRNAs had a larger number of targets, such as the miR482 family (six targets distributed among the 10 family members) (Fig. 9), Aang-novel_19 and Aang-novel20 (six targets), and Aang-novel_63, Aang-novel_94, Aang-novel_95, and Aang-novel_96 with five targets each (Fig. 10, Suppl. Table S5 and S6).

The functional annotation of the 98 unique targets was performed using Trinotate v.3.2.1 pipeline, followed by a GO analysis to evaluate their putative functions regarding the cellular component, molecular function, and biological process (Fig. 11 and Suppl. Table S5 and S6). The majority of miRNA targets identified are localized in the membrane, cytosol, and chloroplast, and some are in the cytoplasm, vacuolar membrane, cytosol, nucleus, ribosome, apoplast, mitochondrion, Golgi apparatus, or plasmodesma (Fig. 11A). Most miRNA targets participate in ATP- and ADP-binding, peptidase activities, RNA binding, kinase activities, glucosidase activities, UDP-glycosyltransferase activities, or ubiquitin-protein transferase activity (Fig. 11B). Interestingly, most targets are involved in defense response and have a broad range of physiological functions. Among them, proteolysis, signal transduction, carbohydrate metabolism,

mRNA processing, response to brassinosteroid, phosphorylation process, DNA methylation. Notably, we also found targets related to embryo development ending seed dormancy (Fig. 11C).

Expression Analysis Of Mirnas And Their Targets By Rt-qpcr

The expression of 11 selected miRNAs (novel and conserved) and 8 corresponding target transcripts were validated by RT-qPCR (primers are shown in Suppl. Table S8 and S9). For the miRNAs miR156*, miR169, and miR536, no target was identified or the target sequences were not complete or showed only a short sequence.

As shown in Suppl. Fig. S6, the expression levels of miR134, miR156*, miR169, miR482, and Aang-34 assayed by RT-qPCR were very similar to the profiles from the sequencing data, mainly miR169 (Suppl. Fig. S6E). The expression pattern of miR1030 and miR536 was similar in Responsive cell lines, whereas the expression of miR394 and Aang-120 (Suppl. Fig. S6B and S6I) were contrasting between stem-loop RT-qPCR and small RNA sequencing, possibly because of the difference in sensitivity between these two technologies (Lin et al. 2020).

The analysis of miRNA and mRNA expression profiles revealed functional miRNA-mRNA interaction pairs involved in embryogenesis (Fig. 12). To verify if the corresponding targets are under some post-transcriptional regulation by miRNAs, RT-qPCR was employed in 8 selected targets, and their expression profiles were compared to those observed in miRNA. Three differentially expressed miRNAs and their target genes showed the expected pattern and were negatively correlated in Responsive [miR1030 and its target *PLEIOTROPIC REGULATORY LOCUS1* (*PRL1*) (Fig. 12C); miR1314 and *ACTIVATED DISEASE RESISTANCE 1-Like 1* (*ADR1-Like 1*) (Fig. 12D)] and Blocked [Aang-34 and its target *LEUCINE-RICH REPEAT RECEPTOR-LIKE PROTEIN KINASE* (*LRR-RK*) (Fig. 12E)] cell lines during the transition from proliferation to the maturation stage. Concerning the remaining miRNAs and targets analyzed, the expression of miR394 in both cell lines were differentially expressed during the transition from proliferation to maturation but their corresponding target *CMP-sialic acid transporter 1* (*CMP*) did not (Fig. 12A). Similar profiles were observed in the expression of miR482 and its target *PENTATRICOPEPTIDE REPEAT-CONTAINING PROTEIN* (*RPF3*) in the Responsive cell line (Fig. 12B), and miR1314 and their targets *ADR1-Like 1* and *Multidrug and Toxic Compound Extrusion or Multi-Antimicrobial Extrusion* (*MATE efflux*) (Fig. 12D). Otherwise, miR1030 was not differentially expressed during this transition in Blocked cell line, but their target TWIN2 increased its expression during the maturation step (Fig. 12G).

The two cell lines were also compared at each embryogenesis stage, aiming to identify differential expression profiles between proliferation and maturation. miR1314 (Suppl. Figure 7D) and Aang-133/135 (Suppl. Figure 7G) were more expressed in the Blocked than Responsive cell line during the proliferation stage, whereas Aang-120 (Suppl. Figure 7F) was less expressed in this comparison. The expression of *ADR1-Like 1* (target gene of miR1314) was lower (Suppl. Figure 7D), and *CALPAIN-TYPE CYSTEINE PROTEASE DEFECTIVE KERNEL 1* (*DEK1*) (targeted by Aang-120) and *LRR* (targeted by Aang-34) were higher in the Blocked cell line (Suppl. Figure 7E, F). *VALINE–tRNA LIGASE MITOCHONDRIAL 1* (*TWIN2*) (targeted by Aang-133/135) expression was similar between the two cell lines (Fig. 12G).

During the maturation stage, six miRNAs (miR394, miR482, miR1030, miR1314, Aang-34, and Aang-120) had lower expression in the Blocked cell line compared to the Responsive cell line. Among the targets, the gene *PRL1* was more expressed in the Blocked cell line (Suppl. Figure 7C), whereas the expression of *LRR, MATE, ADR1-like 1* and *DEK1* were higher in the Responsive cell line (Suppl. Figure 7D, E, F). The other targets did not show significant differences in expression between the cell lines. Putative targets were not identified for miR156*, miR169, and miR536, which showed the highest expression values in RM (Fig. 12H). We also constructed a model to show how the regulation of differentially expressed miRNAs and their corresponding targets are related to both somatic embryogenesis stages and embryogenic potential which are discussed below.

Discussion

The advent of deep sequencing technologies has enabled the identification of miRNAs during embryogenesis in non-model plant species, including conifers (Zhang et al. 2012; Singh et al. 2018; Lin et al. 2020). However, only four conifer species have miRNAs deposited in the miRBase (v22.1) database, and few studies addressed this specific phase of the plant life cycle (Alves et al. 2020), illustrating that our understanding of plant embryogenesis by epigenetics and post-transcriptional regulation is still in its initial moment (Zhang et al. 2012). Here, we performed deep sequencing of small RNA using Illumina technology to identify miRNAs and

evaluate their expression, as well as the regulation of their putative targets, during *A. angustifolia* somatic embryogenesis development.

We identified and annotated 22 conserved miRNAs and 143 high-confidence putative novel miRNAs. These data represent an important source for the study of embryogenesis in conifer species and significantly enrich the current repertoire of published and annotated plant miRNAs. Less than 15% of *A. angustifolia* small RNA reads represented conserved miRNAs. This number is lower compared with the conifer model *Picea abies*, which has more than 600 mature miRNAs identified (Liu and El-Kassaby 2017; available also in miRBase 22.1, Kozomara et al. 2019), but higher when compared to the non-model plants pokeweed (0.5%) and black pepper (11%) (Asha et al. 2016; Neller et al. 2018). Galdino et al. (2019) identified 13 miRNA families in *A. angustifolia*, four of which (miR156, miR169, miR394, and miR1314) also detected in the present study. However, three miRNA families (miR482, miR536, and miR1030) are now described for this species for the first time. These differences probably reflect variations in the experimental and analytical conditions used, such as the type of tissues, plant growth conditions, annotation criteria, and read-count filtering method. Previous studies demonstrated that miR156, miR169, miR394, and miR482 are highly conserved in angiosperms, Bryophyta, and conifers. miR1030 was also identified in *P. patens* (Axtell et al. 2007), and miR1314 in *P. abies* (Xia et al. 2015)d *densata* (Wan et al. 2012).

A distinct set of miRNAs was observed during the transition from proliferation to maturation stage in both cell lines. As demonstrated for other gymnosperms, this transition occurs only after submitting the embryogenic cultures to a stress condition by the supplementation of sorbitol, ABA, and 1% Gelrite® to the culture medium (Stasolla et al. 2002; de Oliveira et al. 2020; Araujo et al. 2022). This stress promotes the expression, or turning off, of dozens to hundreds genes, transcription factors, and hormonal transduction, leading to embryo development (Méndez-Hernández et al. 2019). Distinct cell lines of *A. angustifolia* differentially respond to these stresses modulating the expression of genes sets (Elbl et al. 2015a, 2022; Navarro et al. 2017; de Oliveira et al. 2018, 2020; Araujo et al. 2022).

In this work, we identified miRNAs and new targets in *A. angustifolia*. Among 98 potential targets for 89 miRNAs, 8 miRNAs (miR482, miR536, miR1314, miR394, miR1030, Aang-120, Aang133/135, and Aang-34) and their corresponding targets were selected using the term ‘embryo’ in the Trinotate/GO annotation analyses and their expression was validated by RT-qPCR.

miR482 of *A. angustifoli*a targets an *RPF3* that encodes a pentatricopeptide repeat (PPR) protein involved in the 5' processing of different mitochondrial mRNAs. This protein contributes to post-transcriptional processes (Stoll et al. 2015) and plays important roles in the circadian clock, seed development and germination, and embryogenesis in *A. thaliana* and maize (Oguchi et al. 2004; Gutierrez-Marcos et al. 2007; Yang et al. 2011; Park et al. 2014). Wang et al. (2022) have demonstrated that the gene *MITOCHONDRIAL STABILITY FACTOR 3* (*MTSF3*) encoding a PPR protein is localized in the mitochondrion and its mutation induces embryonic lethality, but this condition could be reverted by partial complementation with the *ABSCISIC ACID INSENSITIVE3* (*ABI3*) promoter. In our study, the miR482 exhibited an increased level of expression during RP-RM transition, suggesting a role in the early somatic embryo evolution in responsive cell lines.

The function of miR536 is still poorly understood, although it has been identified in different plant species: *Larix leptolepis* (Zhang et al. 2013), *Cocos nucifera* (Sabana et al. 2020), *Asparagus officinalis* (Harkess et al. 2017), *Selaginella moellendorffii* and *P. patens* (Axtell et al. 2007). In *P. patens*, transcription factors such as *ABI3* and F-box encoding mRNA, were reported to be potentially regulated by miR536 (Axtell et al. 2007, Xia et al. 2016). Although its potential target was not detected in the *A. angustifolia* transcriptome database (Elbl et al. 2015a), the expression of miR536 significantly increased during RP-RM transition of embryogenic cultures (Fig. 12H). In contrast, lower expression levels were observed for this miRNA in blocked cell lines. These results suggest an association between miR536 and embryogenic potential in *A. angustifolia*, which requires further investigation.

miR1314 has two potential targets: *Multidrug and Toxic Compound Extrusion or Multi-Antimicrobial Extrusion* (*MATE efflux*) and *ADR1-like*. *MATE* transporters comprise a universal gene family of membrane effluxers present in all life kingdoms (Santos et al. 2017), implicated in the transport of different plant regulators, such as salicylic acid, ABA, and auxin (Serrano et al. 2013; Yamasaki et al. 2013; Zhang et al. 2014b; Santos et al. 2017; Kovinich et al. 2018). At the maturation stage, *MATE* is expressed at high levels in the RM cell line (Fig. 12D), when ABA is supplemented to the medium to induce somatic embryos development (Jo et al. 2014; de Oliveira et al. 2018, 2020). These results suggest a possible interaction between ABA and *MATE* expression during somatic embryogenesis. The other potential miR1314-target, *ADR1-Like*, encodes a nucleotide-binding leucine-rich repeat protein (NLR) that contains domains of homology with serine/threonine protein kinases, involved mainly in defense response to pathogens and drought tolerance (Chini et al. 2004; Dong et al. 2016). During RP-RM transition, we observed an increase in *miR1314* expression and a reduced level of its target

ADR1-Like, suggesting that post-transcriptional regulation of *ADR1-like* by miR1314 might be associated with ABA in responsive cell lines. In *adr1* double mutants of *A. thaliana*, an interaction among ADR1-like, salicylic acid, and ABA insensitive1 (ABI1) was correlated with drought stress (Chini et al. 2004).

In *A. angustifolia*, miR394 probably targets a member of the CMP-SIALIC ACID TRANSPORTER 1/NUCLEOTIDE-SUGAR TRANSPORTER (NSTs) family. Genes encoding CMP-sialic acid transporter are poorly characterized in plants, however, the alignment with *A. angustifolia* transcript against Viridiplantae indicated a possible nucleotide-sugar transporter family protein function (Takashima et al. 2009). The *A. thaliana* genome contains more than 40 members of the NSTs family, of which only a few are functionally characterized, acting on transport of nucleotide-sugars from the cytoplasm to the endoplasmic reticulum and Golgi lumen (Bakker et al. 2008). Therefore, to date, the role of these proteins in embryo development is unknown.

miR1030 has annotations only for the moss *P. patens* in the miRBase (Axtell et al. 2007)d *sativa* (Zhou et al. 2010). In *A. angustifolia*, a transcript encoding *PRL1* was identified as a potential target of miR1030. Among its several functions, PRL1 could be involved in the accumulation of miRNAs by stabilizing pri-miRNAs through its RNA-binding activity and enhancing Dicer-Like 1 activity (Zhang et al. 2014a; Wang et al. 2020). In addition, this protein is related to stress, hormone responses, and sugar metabolism, through repression of SnRK1, which is activated upon sugar deprivation (Flores-Pérez et al. 2010; Navarro et al. 2017; Wang et al. 2020). In these same distinct embryogenic potential cell lines of *A. angustifolia*, Navarro et al. (2017) demonstrated that the sugar levels were inversely associated with *SnRK1* expression profile during the maturation stage. Therefore, a possible modulation of gene expression by the complex miR1030-*PRL1-SnRK1* might act during the proliferation to maturation transition in this species. Besides its association with carbohydrate metabolism, PRL1 could be involved in auxin signaling by regulating expression levels of PIN auxin efflux carriers (Ji et al. 2015). In addition, PRL1 is required for the confined expression of the homeodomain transcription factor *WUSCHEL-RELATED HOMEOBOX 5* (*WOX5*) in the quiescent center, and its loss of function promotes premature stem cell differentiation, aberrant cell division, and reduced root meristem size in *A. thaliana* (Ji et al. 2015). Transcriptome analysis of *A. angustifolia* revealed that abnormal somatic embryos have an incorrect auxin distribution and transduction promoted by high *WOX5* expression during the maturation stage (Elbl et al. 2015a). We suggest that *PRL1* could be acting on the regulation of *WOX* genes and auxin signaling in this species.

In this study, we identified the novel miRNA Aang-120 in *A. angustifolia* that possibly targets a transcript encoding for the DEK1 protein. *dek1* mutants of *A. thaliana* have irregular mitotic divisions and arrested embryo development at the globular stage (Lid et al. 2005). In maize and Arabidopsis, DEK1 participates in cell-to-cell communication in epidermal cell fate specification, through a predicted membrane-targeting signal located in the plasma membrane (Lid et al. 2002; Tian et al. 2007). These two contrasting embryogenic cell lines of *A. angustifolia* have differential cell-to-cell trafficking patterns (Navarro et al. 2022), which could be under post-transcriptional regulation related to Aang-novel_120 and *DEK1*.

The miRNAs Aang-novel_133 and Aang-novel_135 were predicted to target the *TWIN2* gene in *A. angustifolia*, which encodes a Valine–tRNA ligase mitochondrial 1. *A. thaliana twin2* mutants exhibited a defect in early embryogenesis. After one or two divisions of the zygote, the apical cell decedents arrest and there is a lack of maintaining suspensor cell identity, with basal cells showing abnormal proliferation (Zhang and Somerville 1997). *TWIN2* was highly expressed during the maturation stage in both cell lines of *A. angustifolia* (Fig. 12G), however, more expressed in BP than RP during proliferation, suggesting its association with initial somatic development.

The Aang-novel_34 targets an *LRR* gene described to encode a PROBABLE INACTIVE LEUCINE-RICH REPEAT RECEPTOR KINASE XIAO protein (Jiang et al. 2012). As observed in rice, soybean, and Arabidopsis, this gene was expressed during seed development and plays a role in the regulation of certain cellular processes that lead to cell division, elongation, and expansion by regulating brassinosteroid signaling (Kim et al. 2009; Jiang et al. 2012). In *A. angustifolia*, during the transition BP-BM, an opposite expression profile between miRNA Aang-novel_34 and the putative *LRR* transcript was observed (Fig. 12E), suggesting an interaction between embryogenic potential and brassinosteroid signaling during embryogenesis.

Conclusions

The present work is the first attempt to integrate miRNA and mRNA expression data to identify key regulatory miRNA-mRNA modules during the *A. angustifolia* somatic embryogenesis, a non-model species belonging to an evolutionarily basal conifer family. A total of 165 miRNAs, 22 known and 143 novels, were identified in two cell lines with contrasting embryogenic potential. Differential expression

was detected for 91 miRNAs, mainly during the proliferation to maturation transition. Among these, 16 were exclusively expressed in RP-RM and 13 in BP-BM transition, indicating that miRNAs probably play important roles in somatic embryo development and might be associated with embryogenic potential. Different miRNAs were predicted to regulate target genes involved in post-transcriptional regulation, ABA and auxin signaling, carbohydrate metabolism, transporters, cell-to-cell communication, and cell identity. The functions and regulatory mechanisms of these miRNAs should be investigated in more detail. Our findings not only provide new insights into miRNA-mediated regulation in *A. angustifolia* somatic embryogenesis but also form a foundation for further research to elucidate the functions of these putative miRNA-target modules in embryogenesis of conifers.

Declarations

Acknowledgments We thank Tiago de Souza and Jonas Gaiarsa (www.taugc.com) for technical support with the bioinformatic analysis, Prof. Dr. Luiz Lehmann Coutinho's group (Centro de Genômica Funcional, ESALQ/USP) for support with sequencing analysis, in Press (https://inpresscientifica.com.br/) for editing this manuscript, and MSc Amanda F. Macedo (University of São Paulo) for technical support with the experimental analysis.

Author contributions LFO and EISF designed the study. LFO carried out the experiments. LFO and ARP carried out the bioinformatic analysis. All authors wrote and approved the final manuscript.

Funding This work was supported by the State of Sao Paulo Research Foundation (FAPESP) [2018/08215-0 to L.F.O., 2020/03791-2 to A.R.P.]; the National Council of Technological and Scientific Development (CNPq) [303606/2017-7]; and the Coordenação de Aperfeiçoamento de Pessoal de Nível Superior-Brasil (CAPES)-Finance Code 001".

Data availability Raw sequencing files of sRNAs reads are publicly available and deposited on NCBI under accession number (will be deposited at an appropriate time).

Conflict of interest The authors declare that they have no conflicts of interest.

References

1. Afgan E, Baker D, Batut B, van den Beek M, Bouvier D, Cech M, Chilton J, Clements D, Coraor N, Grüning BA, Guerler A, Hillman-Jackson J, Hiltemann S, Jalili V, Rasche H, Soranzo N, Goecks J, Taylor J, Nekrutenko A, Blankenberg D (2018) The Galaxy platform for accessible, reproducible and collaborative biomedical analyses: 2018 update. Nucleic Acids Res 46(W1):W537–W544. https://doi.org/10.1093/nar/gky379
2. Alves A, Rodrigues AS, Miguel C (2020) microRNAs in Plant Embryogenesis. In: Miguel C, Dalmay T, Chaves I (eds) Plant microRNAs. Concepts and Strategies in Plant Sciences. Springer, Cham. https://doi.org/10.1007/978-3-030-35772-6_6
3. Andrews S (2019) FastQC: a quality control tool for high throughput sequence data. Available online at: https://www.bioinformatics.babraham.ac.uk/projects/fastqc
4. Araujo AJB, Cerruti GV, Zuccarelli R, Ruiz MR, Freschi L, Singh R, Moerschbacher BM, Floh EIS, dos Santos ALW (2022) Proteomic Analysis of S-Nitrosation Sites During Somatic Embryogenesis in Brazilian Pine, *Araucaria angustifolia* (Bertol.) Kuntze. Frontiers in Plant Science 13:902068. https://doi.org/10.3389/fpls.2022.902068
5. Asha S, Sreekumar S, Soniya EV (2016) Unravelling the complexity of microRNA-mediated gene regulation in black pepper (*Piper nigrum* L.) using high-throughput small RNA profiling. Plant Cell Rep 35:53–63. https://doi.org/10.1007/s00299-015-1866-x
6. Axtell MJ, Snyder JA, Bartel DP (2007) Common Functions for Diverse Small RNAs of Land Plants. Plant Cell 19(6):1750–1769. https://doi.org/10.1105/tpc.107.051706
7. Bakker H, Routier F, Ashikov A, Neumann D, Bosch D, Gerardy-Schahn R (2008) A CMP-sialic acid transporter cloned from *Arabidopsis thaliana*. Carbohydr Res 343(12):2148–2152. https://doi.org/10.1016/j.carres.2008.01.010
8. Becwar MR, Noland TL, Wyckoff JL (1989) Maturation, germination, and conversion of Norway spruce (*Picea abies* L.) somatic embryos to plants. In Vitro Cell Dev Biol Plant 26:575–580. https://doi.org/10.1007/BF02623571
9. Bustin SA, Benes V, Garson JA, Hellemans J, Huggett J, Kubista M, Mueller R, Nolan T, Pfaffl MW, Shipley GL, Vandesompele J, Wittwer CT (2009) The MIQE guidelines: minimum information for publication of quantitative real-time PCR experiments. Clin Chem 55:611–622. https://doi.org/10.1373/clinchem.2008.112797

10. Chini A, Grant JJ, Seki M, Shinozaki K, Loake GJ (2004) Drought tolerance established by enhanced expression of the *CC-NBS-LRR* gene, *ADR1*, requires salicylic acid, EDS1 and ABI1. Plant J 38(5):810 – 22. https://doi.org/10.1111/j.1365-313X.2004.02086.x
11. Chorostecki U, Moro B, Rojas AML, Debernardi JM, Schapire AL, Notredame C, Palatnik JF (2017) Evolutionary footprints reveal insights into plant microRNA biogenesis. Plant Cell 29(6):1248–1261. https://doi.org/10.1105/tpc.17.00272
12. Dai X, Zhao PX (2011) psRNATarget: a plant small RNA target analysis server. Nucleic Acids Res 39:W155–W159. https://doi.org/10.1093/nar/gky316
13. de Oliveira LF, Elbl P, Navarro BV, Macedo AF, dos Santos ALW, Floh EIS (2017) Elucidation of the polyamine biosynthesis pathway during Brazilian pine (*Araucaria angustifolia*) seed development. Tree Physiol 37(1):116–130. https://doi.org/10.1093/treephys/tpw107
14. de Oliveira LF, Navarro BV, Cerruti GV, Elbl P, Minocha R, Minocha SC, dos Santos ALW, Floh EIS (2018) Polyamine- and amino acid-related metabolism: the roles of arginine and ornithine are associated with the embryogenic potential. Plant Cell Physiol 59(5):1084–1098. https://doi.org/10.1093/pcp/pcy049
15. de Oliveira LF, dos Santos ALW, Floh EIS (2020) Polyamine and amino acid profiles in immature *Araucaria angustifolia* seeds and their association with embryogenic culture establishment. Trees 34:845–854. https://doi.org/10.1007/s00468-019-01938-y
16. Dong OX, Tong M, Bonardi V, El Kasmi F, Woloshen V, Wünsch LK, Dangl JL, Li X (2016) TNL-mediated immunity in *Arabidopsis* requires complex regulation of the redundant *ADR1* gene family. New Phytol 210(3):960–973. https://doi.org/10.1111/nph.13821
17. Durzan DJ (2012) Female parthenogenetic apomixis and androsporogenetic parthenogenesis in embryonal cells of *Araucaria angustifolia*: interpolation of progenesis and asexual heterospory in an artificial sporangium. Sex Plant Reprod 25(3):227–246. https://doi.org/10.1007/s00497-012-0189-0
18. dos Santos ALW, Elbl P, Navarro BV, de Oliveira LF, Salvato F, Balbuena TS, Floh EIS (2016) Quantitative proteomic analysis of *Araucaria angustifolia* (Bertol.) Kuntze cell lines with contrasting embryogenic potential. J Proteom 130:180–189. https://doi.org/10.1016/j.jprot.2015.09.027
19. Elbl P, Lira BS, Andrade SCS, Jo L, dos Santos ALW, Coutinho LL, Floh EIS, Rossi M (2015a) Comparative transcriptome analysis of early somatic embryo formation and seed development in Brazilian pine, *Araucaria angustifolia* (Bertol.) Kuntze. Plant Cell Tiss Org Cult 120:903–915. https://doi.org/10.1007/s11240-014-0523-3
20. Elbl P, Navarro BV, de Oliveira LF, Almeida J, Mosini AC, dos Santos ALW, Rossi M, Floh EIS (2015b) Identification and evaluation of reference genes for quantitative analysis of Brazilian pine (*Araucaria angustifolia* Bertol. Kuntze) gene expression. PLoS ONE 10:e0136714. https://doi.org/10.1371/journal.pone.0136714
21. Elbl PM, de Souza DT, Rosado D, de Oliveira LF, Navarro BV, Matioli SR, Floh EIS (2022) Building an embryo: An auxin gene toolkit for zygotic and somatic embryogenesis in Brazilian pine. Gene 817:146168. https://doi.org/10.1016/j.gene.2021.146168
22. Flores-Pérez U, Pérez-Gil J, Closa M, Wright LP, Botella-Pavía P, Phillips MA, Ferrer A, Gershenzon J, Rodríguez-Concepción M (2010) PLEIOTROPIC REGULATORY LOCUS 1 (PRL1) integrates the regulation of sugar responses with isoprenoid metabolism in *Arabidopsis*. Mol Plant 3:101–112. https://doi.org/10.1093/mp/ssp100
23. Friedländer MR, Mackowiak SD, Li N, Chen W, Rajewsky N (2012) miRDeep2 accurately identifies known and hundreds of novel microRNA genes in seven animal clades. Nucleic Acids Res 40(1):37–52. https://doi.org/10.1093/nar/gkr688
24. Galdino JH, Eguiluz M, Guzman F, Margis R (2019) Novel and conserved mirnas among brazilian pine and other gymnosperms. Front Genet 10:222. https://doi.org/10.3389/fgene.2019.00222
25. Gutiérrez-Marcos JF, Dal Prà M, Giulini A, Costa LM, Gavazzi G, Cordelier S, Sellam O, Tatout C, Paul W, Perez P, Dickinson HG, Consonni G (2007) *empty pericarp4* encodes a mitochondrion-targeted pentatricopeptide repeat protein necessary for seed development and plant growth in maize. Plant Cell 19: 196–210. https://10.1105/tpc.105.039594
26. Harkess A, Zhou J, Xu C et al (2017) The asparagus genome sheds light on the origin and evolution of a young Y chromosome. Nat Commun 8:1279. https://doi.org/10.1038/s41467-017-01064-8
27. Jeena GS, Singh N, Shikha, Shukla RK (2022) An insight into microRNA biogenesis and its regulatory role in plant secondary metabolism. Plant Cell Rep 41(8):1651–1671. https://doi.org/10.1007/s00299-022-02877-8
28. Ji H, Wang S, Li K, Szakonyi D, Koncz C, Li X (2015) PRL1 modulates root stem cell niche activity and meristem size through *WOX5* and *PLTs* in Arabidopsis. Plant J 81(3):399–412. https://doi.org/10.1111/tpj.12733
29. Jiang Y, Bao L, Jeong SY, Kim SK, Xu C, Li X, Zhang Q (2012) XIAO is involved in the control of organ size by contributing to the regulation of signaling and homeostasis of brassinosteroids and cell cycling in rice. Plant J 2012;70(3):398–408.

https://doi.org/10.1111/j.1365-313X.2011.04877.x

30. Jo L, dos Santos ALW, Bueno CA, Barbosa HR, Floh EIS (2014) Proteomic analysis and polyamines, ethylene and reactive oxygen species levels of *Araucaria angustifolia* (Brazilian pine) embryogenic cultures with different embryogenic potential. Tree Physiol 34:94–104. https://doi.org/10.1093/treephys/tpt102
31. Juárez-González VT, López-Ruiz BA, Baldrich P, Luján-Soto E, Meyers BC, Dinkova TD (2019) The explant developmental stage profoundly impacts small RNA-mediated regulation at the dedifferentiation step of maize somatic embryogenesis. Sci Rep 9:14511. https://doi.org/10.1038/s41598-019-50962-y
32. Kim S, Kim SJ, Shin YJ, Kang JH, Kim MR, Nam KH, Lee MS, Lee SH, Kim YH, Hong SK, Verma DP, Chun JY, Cheon CI (2009) An atypical soybean leucine-rich repeat receptor-like kinase, *GmLRK1*, may be involved in the regulation of cell elongation. Planta 229(4):811–821. https://doi.org/10.1007/s00425-008-0873-3
33. Köster T, Meyer K, Weinholdt C, Smith LM, Lummer M, Speth C, Grosse I, Weigel D, Staiger D (2014) Regulation of pri-miRNA processing by the hnRNP-like protein *AtGRP7* in Arabidopsis. Nucleic Acids Res 42(15):9925–9936. https://doi.org/10.1093/nar/gku716
34. Kovinich N, Wang Y, Adegboye J, Chanoca AA, Otegui MS, Durkin P, Grotewold E (2018) Arabidopsis MATE45 antagonizes local abscisic acid signaling to mediate development and abiotic stress responses. Plant Direct 2(10):e00087. https://doi.org/10.1002/pld3.87
35. Kozomara A, Birgaoanu M, Griffiths-Jones S (2019) miRBase: form microRNA sequences to function. Nucleic Acids Res 47:D155–D162. https://doi.org/10.1093/nar/gky1141
36. Lakhwani D, Sanchita, Pandey A, Sharma D, Asif MH, Trivedi PK (2020) Novel microRNAs regulating ripening-associated processes in banana fruit. Plant Growth Regul 90:223–235. https://doi.org/10.1007/s10725-020-00572-w
37. Langmead B, Trapnell C, Pop M, Salzberg SL (2009) Ultrafast and memory-efficient alignment of short DNA sequences to the human genome. Genome Biol 10:R25. https://doi.org/10.1186/gb-2009-10-3-r25
38. Li Q, Deng C, Xia Y, Kong L, Zhang H, Zhang S, Wang J (2017) Identification of novel miRNAs and miRNA expression profiling in embryogenic tissues of *Picea balfouriana* treated by 6-benzylaminopurine. PLoS ONE 12(5):e0176112. https://doi.org/10.1371/journal.pone.0176112
39. Lid SE, Gruis D, Jung R, Lorentzen JA, Ananiev E, Chamberlin M, Niu X, Meeley R, Nichols S, Olsen O-A (2002) The *defective kernel 1* (*dek1*) gene required for aleurone cell development in the endosperm of maize grains encodes a membrane protein of the calpain gene superfamily. PNAS 99(8):5460–5465. https://doi.org/10.1073/pnas.042098799
40. Lid SE, Olsen L, Nestestog R, Aukerman M, Brown RC, Lemmon B, Mucha M, Opsahl-Sorteberg HG, Olsen OA (2005) Mutation in the *Arabidopisis thaliana* DEK1 calpain gene perturbs endosperm and embryo development while over-expression affects organ development globally. Planta 221:339–351. https://doi.org/10.1007/s00425-004-1448-6
41. Lin S, Su S, Jin L, Peng R, Sun D, Ji H, Yu Y, Xu J (2020) Identification of microRNAs and their targets in inflorescences of an Ogura-type cytoplasmic male-sterile line and its maintainer fertile line of turnip (*Brassica rapa* ssp. *rapifera*) via high-throughput sequencing and degradome analysis. PLoS ONE 15(7):e0236829. https://doi.org/10.1371/journal.pone.0236829
42. Liu Y, El-Kassaby YA (2017) Landscape of fluid sets of hairpin-derived 21-/24-nt-long small RNAs at seed set uncovers special epigenetic features in *Picea glauca*. Genome Biol Evol 9:82–92. https://doi.org/10.1093/gbe/evw283
43. Liu X, Zhang X, Sun B, Hao L, Liu C, Zhang D, Tang H, Li C, Li Y, Shi Y, Xie X, Song Y, Wang T, Li Y (2019) Genome-wide identification and comparative analysis of drought-related microRNAs in two maize inbred lines with contrasting drought tolerance by deep sequencing. PLoS ONE 14(7):e0219176. https://doi.org/10.1371/journal.pone.0219176
44. Martin M (2011) Cutadapt removes adapter sequences from high-throughput sequencing reads. EMBnet J 17(1). https://doi.org/10.14806/ej.17.1.200
45. Méndez-Hernández HA, Ledezma-Rodríguez M, Avilez-Montalvo RN, Juárez-Gómez YL, Skeete A, Avilez-Montalvo J, De-la-Peña C, Loyola-Vargas VM (2019) Signaling Overview of Plant Somatic Embryogenesis. Front Plant Sci 10:77. https://doi.org/10.3389/fpls.2019.00077
46. Navarro BV, Elbl P, De Souza AP, Jardim V, de Oliveira LF, Macedo AF, Dos Santos ALW, Buckeridge MS, Floh EIS (2017) Carbohydrate-mediated responses during zygotic and early somatic embryogenesis in the endangered conifer, *Araucaria angustifolia*. PLoS ONE 12:e0180051. https://doi.org/10.1371/journal.pone.0180051

47. Navarro BV, Elbl P, de Oliveira LF, Piovezani A, dos Santos ALW, de Souza DT, Demarco D, Buckeridge MS, Floh EIS (2022) Cell-to-cell trafficking patterns in cell lines of *Araucaria angustifolia* (Brazilian pine) with contrasting embryogenic potential. Plant Cell Tiss Organ Cult 148:81–93. https://doi.org/10.1007/s11240-021-02166-4
48. Neller KCM, Klenov A, Guzman JC, Hudak KA (2018) Integration of the pokeweed miRNA and mRNA transcriptomes reveals targeting of jasmonic acid-responsive genes. Front Plant Sci 9:589. https://doi.org/10.3389/fpls.2018.00589
49. Oguchi T, Sage-Ono K, Kamada H, Ono M (2004) Genomic structure of a novel *Arabidopsis* clock-controlled gene, *AtC401*, which encodes a pentatricopeptide repeat protein. Gene 330:29–37. https://doi.org/10.1016/j.gene.2003.11.012
50. Park YJ, Lee HJ, Kwak KJ, Lee K, Hong SW, Kang H (2014) MicroRNA400-guided cleavage of Pentatricopeptide repeat protein mRNAs Renders *Arabidopsis thaliana* more susceptible to pathogenic bacteria and fungi. Plant Cell Physiol 55(9):1660–1668. https://doi.org/10.1093/pcp/pcu096
51. Plotnikova A, Kellner MJ, Schon MA, Mosiolek M, Nodine MD (2019) MicroRNA dynamics and functions during Arabidopsis embryogenesis. Plant Cell 31(12):2929–2946. https://doi.org/10.1105/tpc.19.00395
52. Robinson MD, McCarthy DJ, Smyth GK (2010) edgeR: a Bioconductor package for differential expression analysis of digital gene expression data. Bioinformatics 26(1):139–140. https://doi.org/10.1093/bioinformatics/btp616
53. Rodrigues AS, Chaves I, Costa BV, Lin YC, Lopes S, Milhinhos A, Van de Peer Y, Miguel CM (2019) Small RNA profiling in *Pinus pinaster* reveals the transcriptome of developing seeds and highlights differences between zygotic and somatic embryos. Sci Rep 9:11327. https://doi.org/10.1038/s41598-019-47789-y
54. Rogers K, Chen X (2013) Biogenesis, turnover, and mode of action of plant microRNAs. Plant Cell 25(7):2383–2399. https://doi.org/10.1105/tpc.113.113159
55. Ruijter JM, Ramakers C, Hoogaars WM, Karlen Y, Bakker O, van den Hoff MJ, Moorman AF (2009) Amplification efficiency: linking baseline and bias in the analysis of quantitative PCR data. Nucleic Acids Res 37:e45. https://doi.org/10.1093/nar/gkp045
56. Sabana AA, Rajesh MK, Antony G (2020) Dynamic changes in the expression pattern of miRNAs and associated target genes during coconut somatic embryogenesis. Planta 251:79. https://doi.org/10.1007/s00425-020-03368-4
57. Santos ALD, Chaves-Silva S, Yang L, Maia LGS, Chalfun-Júnior A, Sinharoy S, Zhao J, Benedito VA (2017) Global analysis of the MATE gene family of metabolite transporters in tomato. BMC Plant Biol 17(1):185. https://doi.org/10.1186/s12870-017-1115-2
58. Schlögl PS, dos Santos ALW, Vieira LN, Floh EIS, Guerra MP (2012a) Cloning and expression of embryogenesis-regulating genes in *Araucaria angustifolia* (Bert.) O. Kuntze (Brazilian pine). Genet Mol Biol 35:172–181. https://doi.org/10.1590/S1415-47572012005000005
59. Schlögl PS, dos Santos ALW, Vieira LN, Floh EIS, Guerra MP (2012b) Gene expression during early somatic embryogenesis in Brazilian pine (*Araucaria angustifolia* (Bert) O. Ktze). Plant Cell Tiss Organ Cult 108:173–180. https://doi.org/10.1007/s11240-011-0023-7
60. Serrano M, Wang B, Aryal B, Garcion C, Abou-Mansour E, Heck S, Geisler M, Mauch F, Nawrath C, Métraux J-P (2013) Export of salicylic acid from the chloroplast requires the multidrug and toxin extrusion-like transporter EDS5. Plant Physiol 162(4):1815–1821. https://doi.org/10.1104/pp.113.218156
61. Siddiqui ZH, Abbas ZK, Ansari MW, Khan MN (2019) The role of miRNA in somatic embryogenesis. Genomics 111(5):1026–1033. https://doi.org/10.1016/j.ygeno.2018.11.022
62. Singh A, Gautam V, Singh S, Sarkar Das S, Verma S, Mishra V, Mukherjee S, Sarkar AK (2018) Plant small RNAs: advancement in the understanding of biogenesis and role in plant development. Planta 248:545–558. https://doi.org/10.1007/s00425-018-2927-5
63. Sparks E, Wachsman G, Benfey PN (2013) Spatiotemporal signaling in plant development. Nat Rev Genet 14:631–644. https://doi.org/10.1038/nrg3541
64. Stasolla C, Kong L, Yeung EC, Thorpe TA (2002) Maturation of somatic embryos in conifers: morphogenesis, physiology, biochemistry, and molecular biology. In Vitro Cell Dev Biol Plant 38:93–105. https://doi.org/10.1079/IVP2001262
65. Stoll K, Jonietz C, Binder S (2015) In *Arabidopsis thaliana* two co-adapted cyto-nuclear systems correlate with distinct *ccmC* transcript sizes. Plant J 81(2):247–257. https://doi.org/10.1111/tpj.12724
66. Streitner C, Köster T, Simpson CG, Shaw P, Danisman S, Brown JW, Staiger D (2012) An hnRNP-like RNA-binding protein affects alternative splicing by *in vivo* interaction with transcripts in *Arabidopsis thaliana*. Nucleic Acids Res 40(22):11240–11255. https://doi.org/10.1093/nar/gks873

67. Tahir M, Law DA, Stasolla C (2006) Molecular characterization of *PgAGO*, a novel conifer gene of the *ARGONAUTE* family expressed in apical cells and required for somatic embryo development in spruce. Tree Physiol 26:1257–1270. https://doi.org/10.1093/treephys/26.10.1257
68. Takashima S, Seino J, Nakano T, Fujiyama K, Tsujimoto M, Ishida N, Hashimoto Y (2009) Analysis of CMP-sialic acid transporter-like proteins in plants. Phytochemistry 70:17–18. 1973–1981. https://doi.org/10.1016/j.phytochem.2009.09.017
69. The RNAcentral Consortium (2019) RNAcentral: a hub of information for non-coding RNA sequences. Nucleic Acids Res 47(D1):D221–D229. https://doi.org/10.1093/nar/gky1034
70. Tian Q, Olsen L, Sun B, Lid SE, Brown RC, Lemmon BE, Fosnes K, Gruis DF, Opsahl-Sorteberg HG, Otegui MS, Olsen OA (2007) Subcellular localization and functional domain studies of DEFECTIVE KERNEL1 in maize and *Arabidopsis* suggest a model for aleurone cell fate specification involving CRINKLY4 and SUPERNUMERARY ALEURONE LAYER1. Plant Cell 19(10):3127–3145. https://doi.org/10.1105/tpc.106.048868
71. Tiwari JK, Buckseth T, Zinta R, Saraswati A, Singh RK, Rawat S, Chakrabarti SK (2020) Genome-wide identification and characterization of microRNAs by small RNA sequencing for low nitrogen stress in potato. PLoS ONE 15(5):e0233076. https://doi.org/10.1371/journal.pone.0233076
72. Varkonyi-Gasic E, Wu R, Wood M, Walton EF, Hellens RP (2007) Protocol: a highly sensitive RT-PCR method for detection and quantification of microRNAs. Plant Methods 3:12. https://doi.org/10.1186/1746-4811-3-12
73. Wan LC, Zhang H, Lu S, Zhang L, Qiu Z, Zhao Y, Zeng QY, Lin J (2012) Transcriptome-wide identification and characterization of miRNAs from *Pinus densata*. BMC Genomics 13:132. https://doi.org/10.1186/1471-2164-13-132
74. Wang C, Blondel L, Quadrado M, Dargel-Graffin C, Mireau H (2022) Pentatricopeptide repeat protein MTSF3 ensures mitochondrial RNA stability and embryogenesis. https://doi.org/10.1093/plphys/kiac309. Plant Physiology kiac309
75. Wang M, Zang L, Jiao F, Perez-Garcia M-D, Ogé L, Hamama L, Le Gourrierec J, Sakr S, Chen J (2020) Sugar Signaling and Post-transcriptional Regulation in Plants: An Overlooked or an Emerging Topic? Front Plant Sci 11:578096. https://doi.org/10.3389/fpls.2020.578096
76. Wei W, Li G, Jiang X, Wang Y, Ma Z, Niu Z, Wang Z, Geng X (2018) Small RNA and degradome profiling involved in seed development and oil synthesis of *Brassica napus*. PLoS ONE 13(10):e0204998. https://doi.org/10.1371/journal.pone.0204998
77. Wójcik AM, Nodine MD, Gaj MD (2017) miR160 and miR166/165 contribute to the *LEC2*-mediated auxin response involved in the somatic embryogenesis induction in Arabidopsis. Front Plant Sci 8:2024. https://doi.org/10.3389/fpls.2017.02024
78. Wójcik AM, Gaj MD (2016) miR393 contributes to the embryogenic transition induced *in vitro* in Arabidopsis via the modification of the tissue sensitivity to auxin treatment. Planta 244:231–243. https://doi.org/10.1007/s00425-016-2505-7
79. Wu XM, Liu MY, Ge XX, Xu Q, Guo WW (2011) Stage and tissue-specific modulation of ten conserved miRNAs and their targets during somatic embryogenesis of Valencia sweet orange. Planta 233:495–505. https://doi.org/10.1007/s00425-010-1312-9
80. Xia J, Wang X, Perroud PF, He Y, Quatrano R, Zhang W (2016) Endogenous Small-Noncoding RNAs and Potential Functions in Desiccation Tolerance in *Physcomitrella Patens*. Sci Rep 6:30118. https://doi.org/10.1038/srep30118
81. Xia R, Xu J, Arikit S, Meyers BC (2015) Extensive families of miRNAs and PHAS loci in Norway Spruce demonstrate the origins of complex phasiRNA networks in seed plants. Mol Biol Evol 32(11):2905–2918. https://doi.org/10.1093/molbev/msv164
82. Xu X, Chen X, Chen Y, Zhang Q, Su L, Chen X, Chen Y, Zhang Z, Lin Y, Lai Z (2020) Genome-wide identification of miRNAs and their targets during early somatic embryogenesis in *Dimocarpus longan* Lour. Sci Rep 10, 4626. https://doi.org/10.1038/s41598-020-60946-y
83. Yamasaki K, Motomura Y, Yagi Y, Nomura H, Kikuchi S, Nakai M, Shiina T (2013) Chloroplast envelope localization of EDS5, an essential factor for salicylic acid biosynthesis in *Arabidopsis thaliana*. Plant Signal Behav 8(4):e23603. https://doi.org/10.4161/psb.23603
84. Yang L, Peng X, Sun MX (2011) *AtNG1* encodes a protein that is required for seed germination. Plant Sci 181:457–464. https://doi.org/10.1016/j.plantsci.2011.07.011
85. Zhang JZ, Somerville CR (1997) Suspensor-derived polyembryony caused by altered expression of valyl-tRNA synthetase in the twn2 mutant of *Arabidopsis*. PNAS 94(14):7349–7355. https://doi.org/10.1073/pnas.94.14.7349
86. Zhang J, Zhang S, Han S, Wu T, Li X, Li W, Qi L (2012) Genome-wide identification of microRNAs in larch and stage-specific modulation of 11 conserved microRNAs and their targets during somatic embryogenesis. Planta 236:647–657. https://doi.org/10.1007/s00425-012-1643-9

87. Zhang J, Zhang S, Han S, Li X, Tong Z, Qi L (2013) Deciphering Small noncoding RNAs during the transition from dormant embryo to germinated embryo in Larches (*Larix leptolepis*). PLoS ONE 8(12):e81452. https://doi.org/10.1371/journal.pone.0081452
88. Zhang R, Jing Y, Zhang H, Niu Y, Liu C, Wang J, Zen K, Zhang C-Y, Li D (2018a) Comprehensive evolutionary analysis of the major RNA-Induced Silencing Complex members. Sci Rep 8:14189. https://doi.org/10.1038/s41598-018-32635-4
89. Zhang Y, Wang Y, Gao X, Liu C, Gai S (2018b) Identification and characterization of microRNAs in tree peony during chilling induced dormancy release by high-throughput sequencing. Sci Rep 8:4537. https://doi.org/10.1038/s41598-018-22415-5
90. Zhang S, Liu Y, Yu B (2014a) PRL1, an RNA-binding protein, positively regulates the accumulation of miRNAs and siRNAs in *Arabidopsis*. PLoS Genet 10:e1004841. https://doi.org/10.1371/journal.pgen.1004841
91. Zhang H, Zhu H, Pan Y, Yu Y, Luan S, Li L (2014b) A DTX/ MATE-type transporter facilitates abscisic acid efflux and modulates ABA sensitivity and drought tolerance in *Arabidopsis*. Mol Plant 7(10):1522–1532. https://doi.org/10.1093/mp/ssu063
92. Zhou L, Liu Y, Liu Z, Kong D, Duan M, Luo L (2010) Genome-wide identification and analysis of drought-responsive microRNAs in *Oryza sativa*. J Exp Bot 61(15):4157–4168. https://doi.org/10.1093/jxb/erq237

Table

Table 1 is available in the Supplementary Files section.

Figures

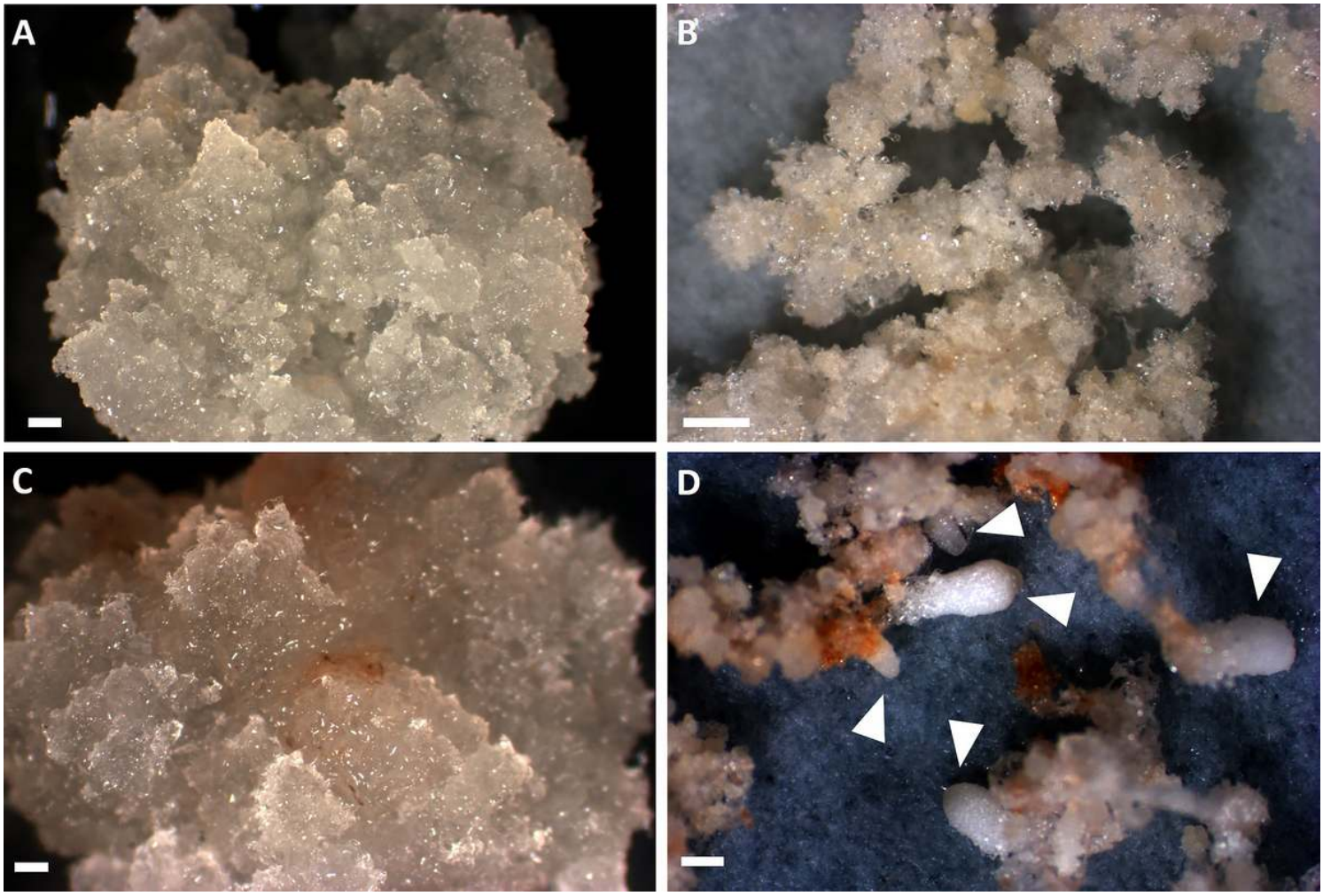

Figure 1

Schematic overview of somatic embryogenesis of *Araucaria angustifolia* protocol in two cell lines with distinct embryogenic potential used in this study: Blocked cell line during the proliferation (**A**) and maturation (**B**) stages; Responsive cell line during the proliferation

(**C**) and maturation (**D**) stages. In (**D**), early somatic embryos (arrows) develop in mature conditions. Scale bar: 1 mm.

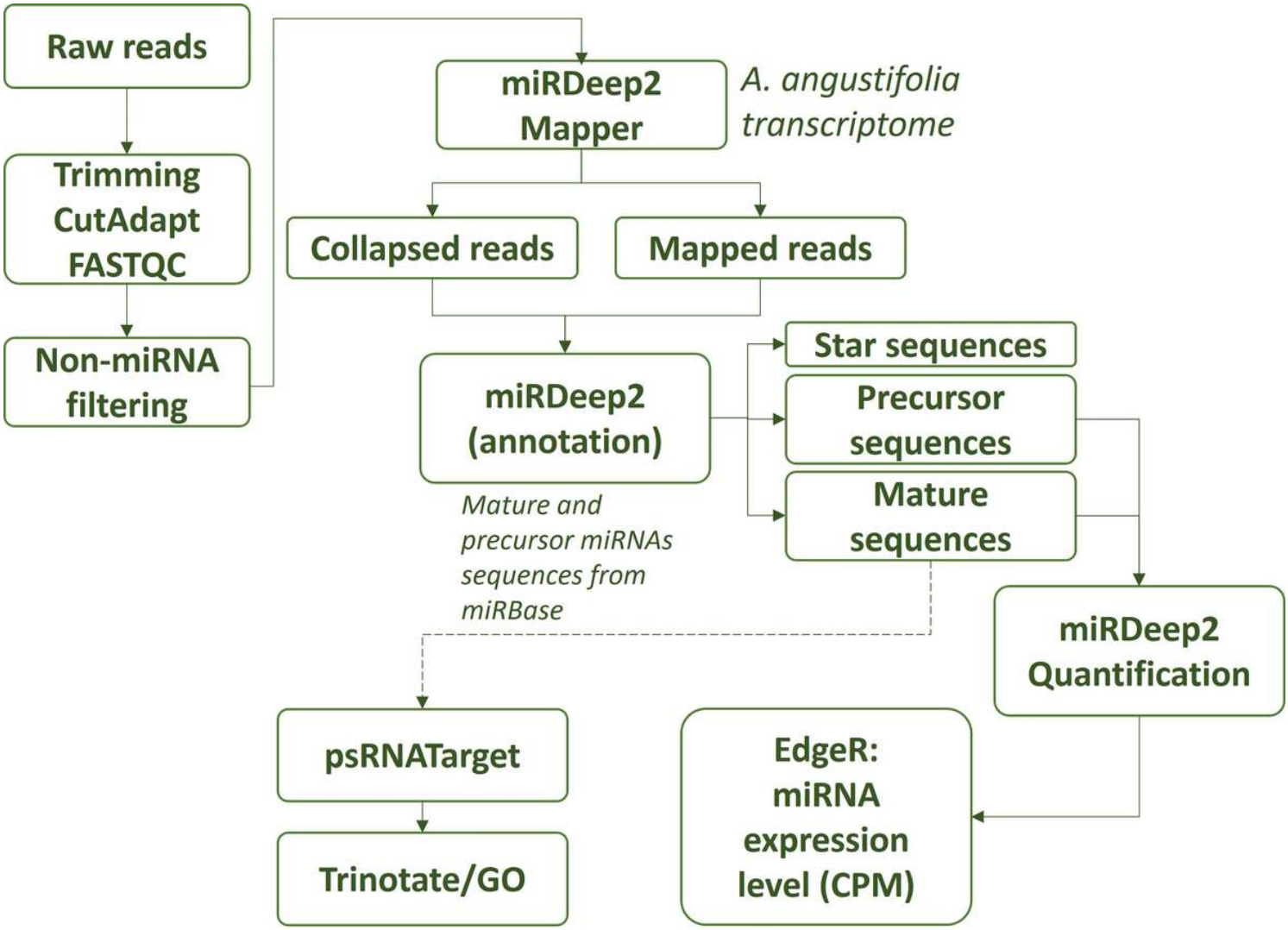

Figure 2

Pipeline for miRNA prediction using miRDeep2, target identification through psRNATarget, differential expression by EdgeR, and function analysis by target annotation through Blast2GO, among the samples group during the somatic embryogenesis of *Araucaria angustifolia*. Briefly, Illumina raw reads were uploaded on FastQC for quality analysis and non-miRNAs were removed. Filtered reads were uploaded on the miRDeep2 mapper module together with the *A. angustifolia* transcriptome (Elbl et al. 2015a) as reference. Collapsed and mapped reads output were used as input on miRDeep2 core together with mature and precursor miRNAs from Viridiplantae from miRbase v22.1. Precursor, mature, and star miRNAs sequences were predicted. The mature miRNA expression level was measured as count per million (CPM). Target prediction was performed by uploading mature miRNA sequences identified in the previous steps and using the *A. angustifolia* transcriptome (Elbl et al. 2015a) as query.

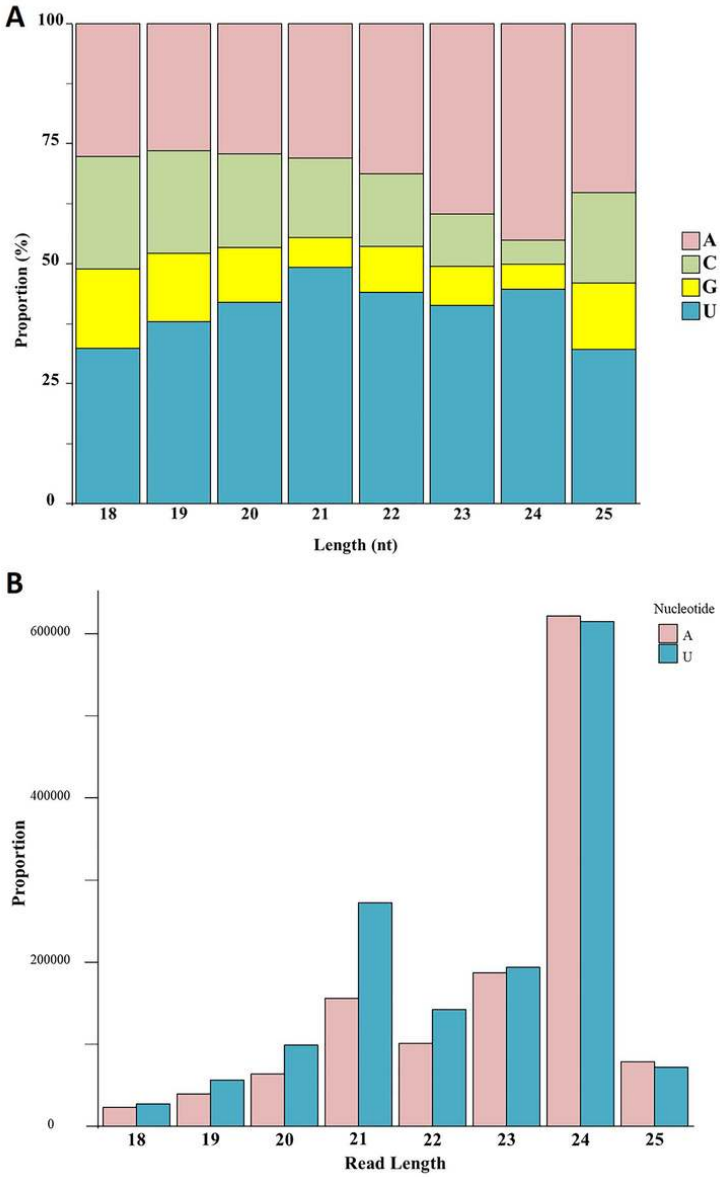

Figure 3

Composition of nucleotides in the first base of sRNA in *Araucaria angustifolia* cell lines. (**A**) The Y-axis displays the proportion of sRNAs with a certain base type as the first base, and the X-axis represents the length classification of the sRNAs. (**B**) Percentage of adenosine or uridine at the start position of 18 to 25-nucleotide (nt) sRNAs. The complete distribution is available in Supplementary Figures S1 and S2. 'A', adenosine; 'C', cytosine; 'G', guanine; 'U', uridine.

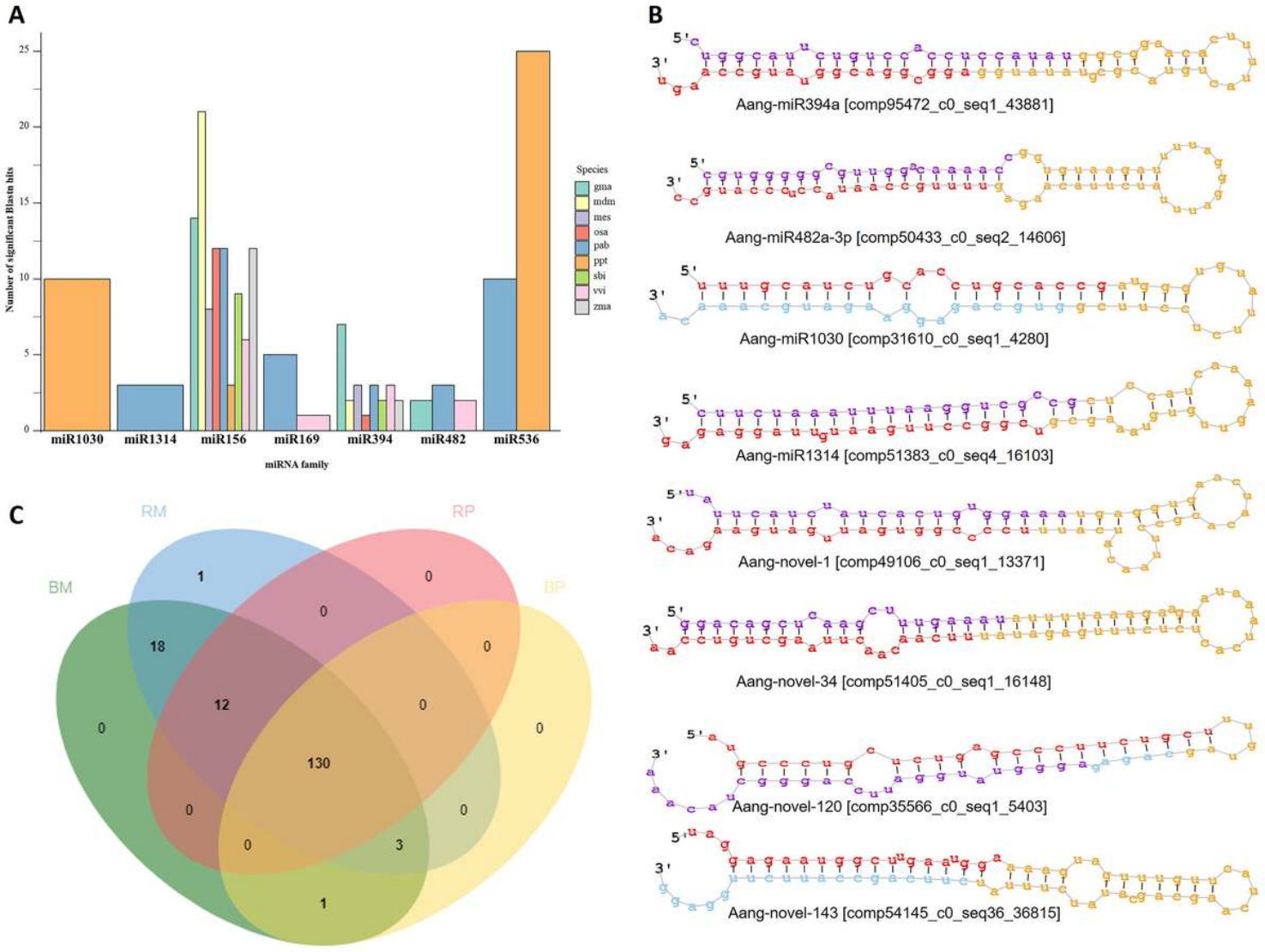

Figure 4

Characterization of global miRNAs identified in *Araucaria angustifolia*. (**A**) Number of paralogs per conserved miRNA family in Viridiplantae species from miRbase v22.1. gma, *Glycine max*; mdm, *Malus domestica*; mes, *Manihot esculenta*; osa, *Oryza sativa*; pab, *Picea abies*; ppt, *Physcomitrella patens*; sbi, *Sorghum bicolor*; vvi, *Vitis vinifera*; zma, *Zea mays*. (**B**) Secondary structures of known and novel miRNAs predicted. Red indicates mature sequence, blue/purple is the star sequence, and yellow represents the loop sequence and part of the arms. Values of the miRNA read counts are presented in Supplementary Tables S3 and S4, and Supplementary Excel File E1. (**C**) Venn diagram of all mature miRNAs identified and their distribution in the four group samples analyzed. RP, responsive cell line in proliferation stage; RM, responsive cell line in maturation stage; BP, blocked cell line in proliferation stage; BM, blocked cell line in maturation stage. Venn diagram comparing the distribution of miRNAs within specific groups is available in Supplementary Figure S4. Exclusive and common miRNAs among the four group samples are listed in Supplementary File E2.

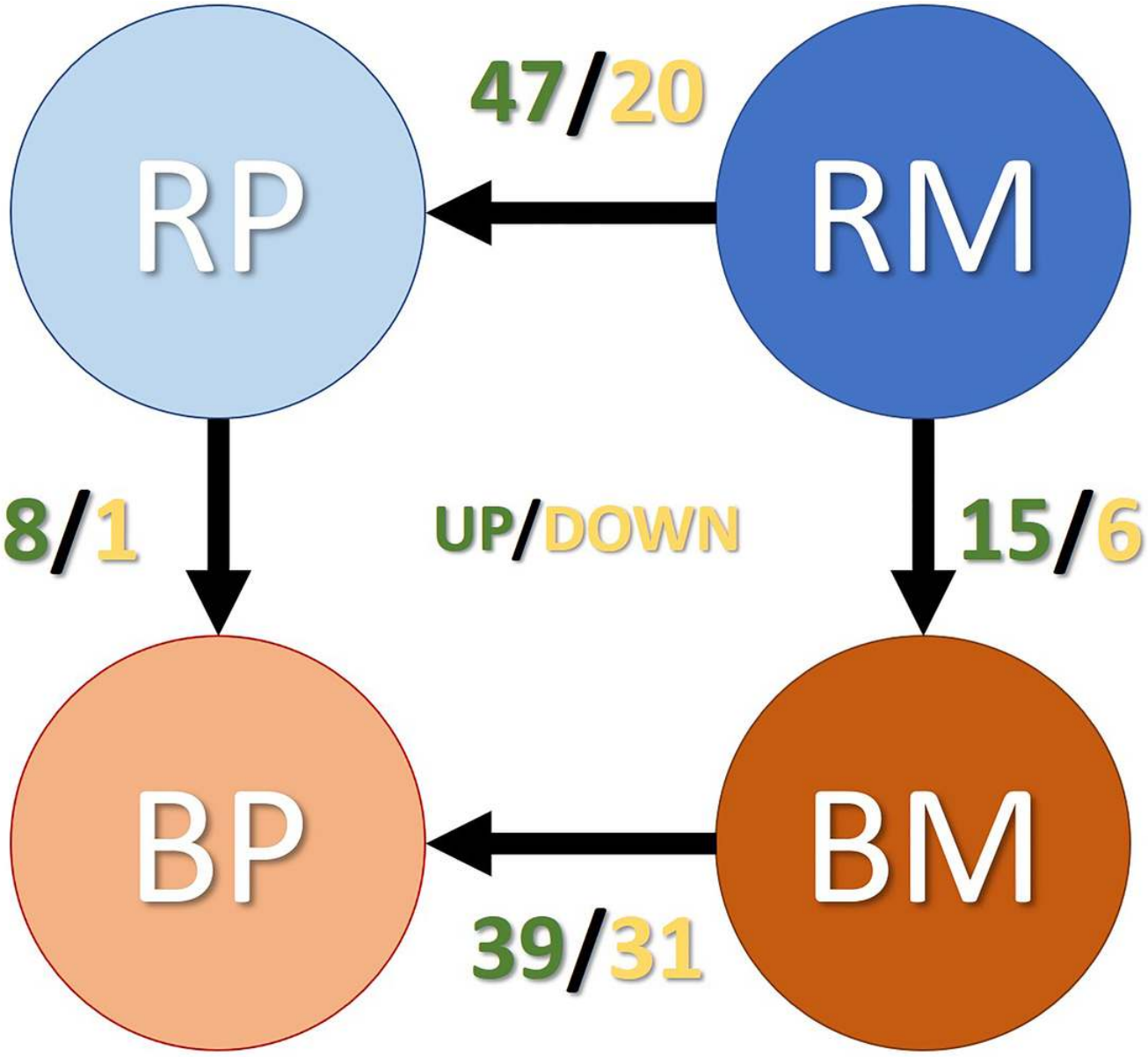

Figure 5

Global view of up- and down-regulated miRNAs among the sample groups during the somatic embryogenesis of *Araucaria angustifolia*. RP, responsive cell line in proliferation stage; RM, responsive cell line in maturation stage; BP, blocked cell line in proliferation stage; BM, blocked cell line in maturation stage. Arrows indicate the order of comparison and the fold changes will be up/down at the start point of the arrow relative to the arrowhead.

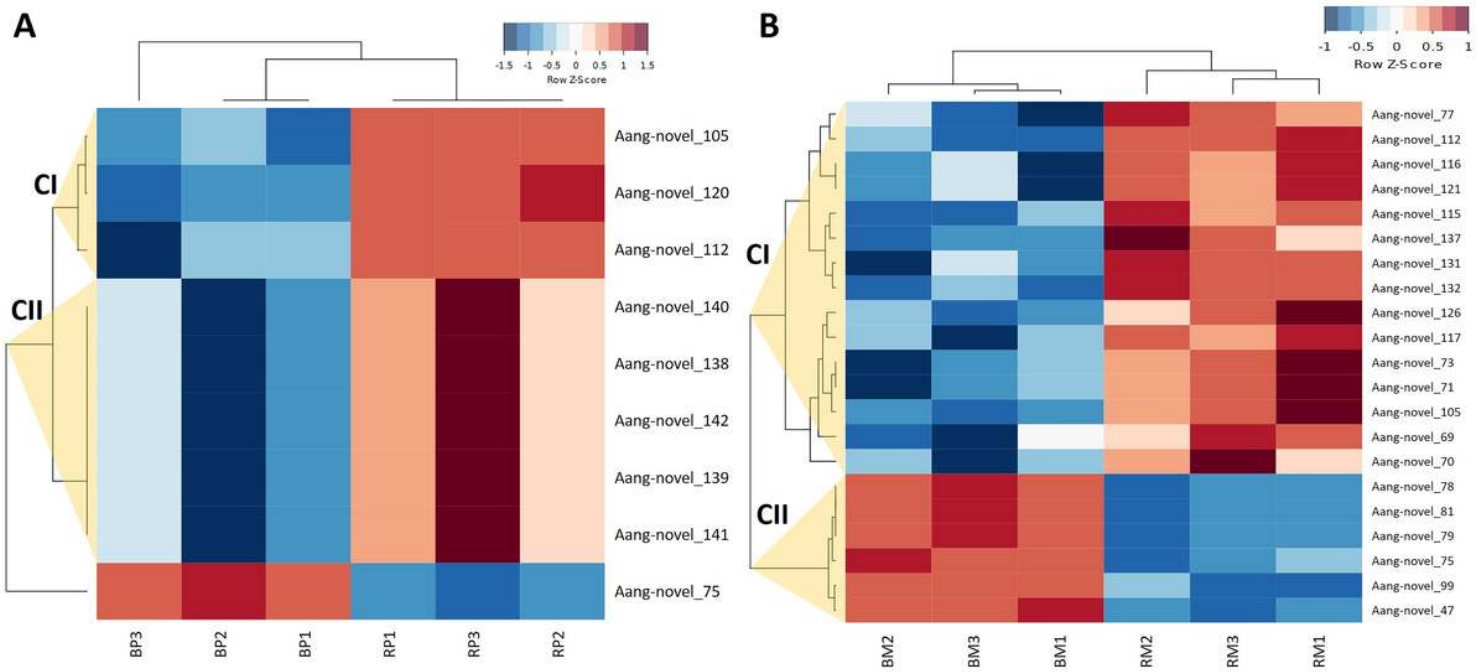

Figure 6

Hierarchical heatmap clustering miRNA expression level between Responsive (RP) and Blocked (BP) cell line during proliferation (**A**) and maturation (**B**) stages in *Araucaria angustifolia* somatic embryogenesis. The heatmap was constructed with miRNAs that were differentially expressed (RP/BP and RM/BM) (*P*-value<0.01; FDR<0.01; LogFC>1.5), after being normalized to the expression of count-per-million (CPM). The blue and red colors indicate a down-regulated and an up-regulated pattern, respectively.

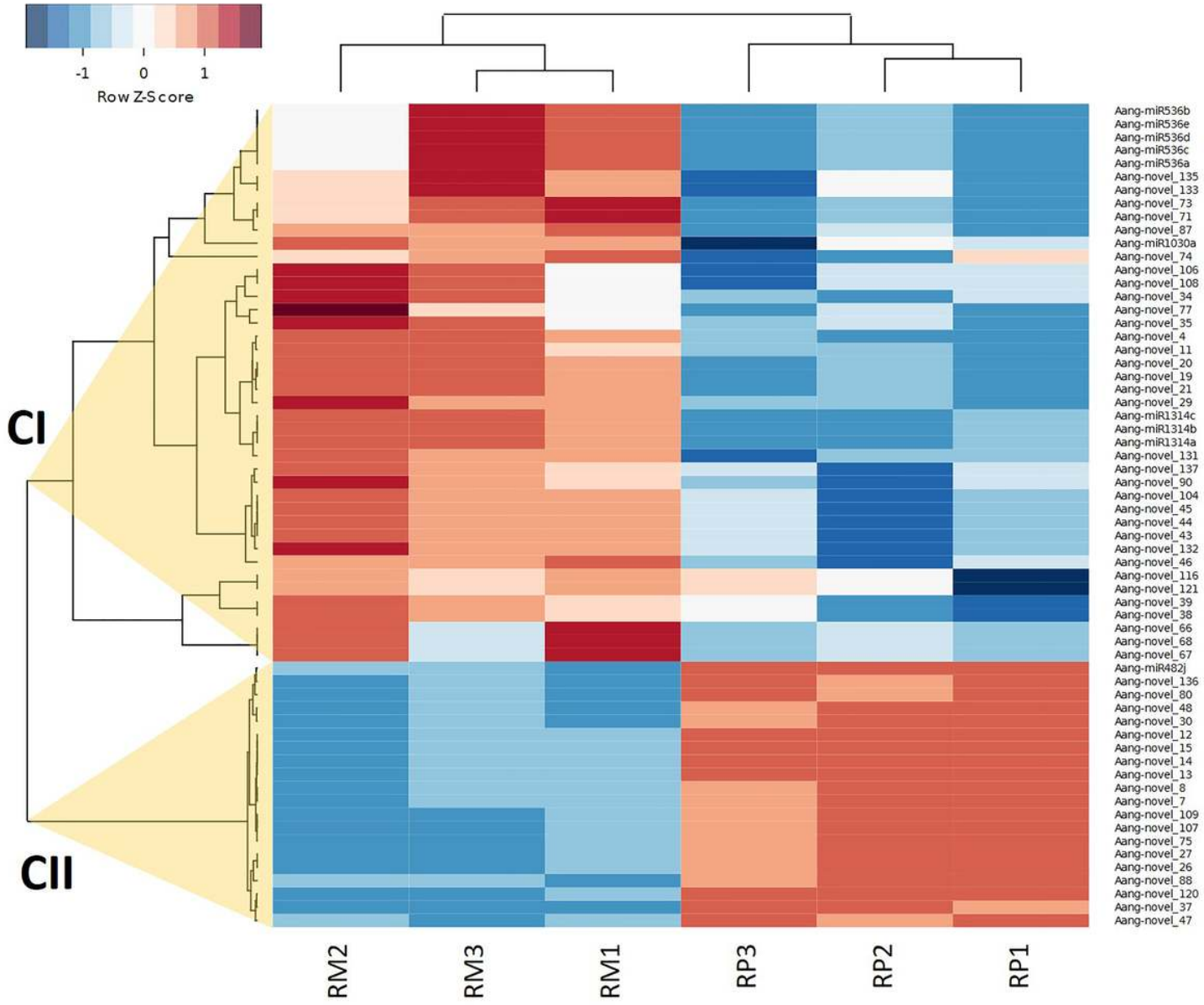

Figure 7

Hierarchical heatmap clustering miRNA expression level in a Responsive cell line of *Araucaria angustifolia* during the transition from proliferation (RP) to maturation (RM) stages of somatic embryogenesis. The heatmap was constructed with miRNAs that were differentially expressed (RM/RP) (*P*-value<0.01; FDR<0.01; LogFC>1.5), after being normalized to the expression of count-per-million (CPM). The blue and red colors indicate a down-regulated and an up-regulated pattern, respectively.

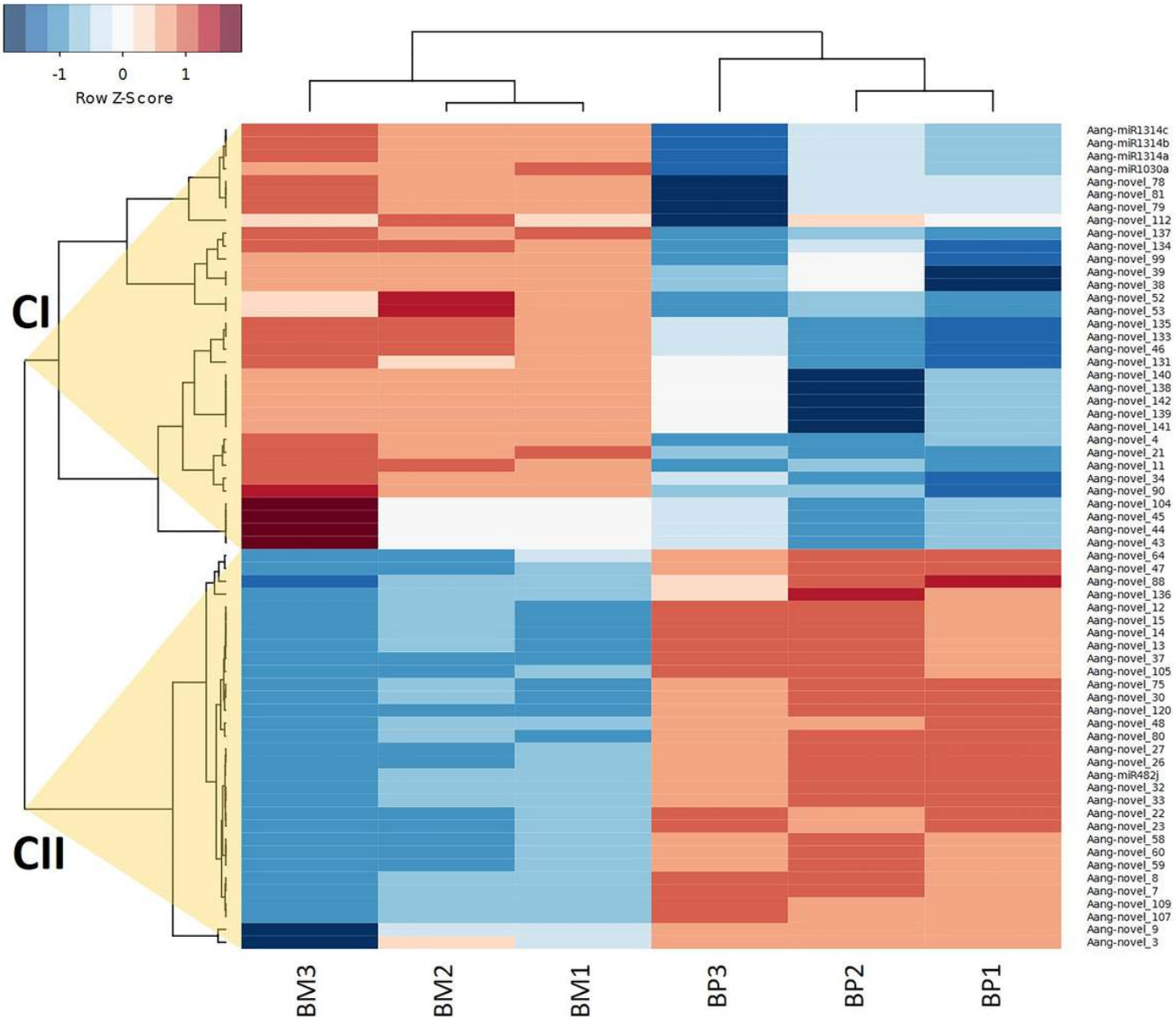

Figure 8

Hierarchical heatmap clustering miRNA expression level in a Blocked cell line of *Araucaria angustifolia* during the transition from proliferation (BP) to maturation (BM) stages of somatic embryogenesis. The heatmap was constructed with miRNAs that were differentially expressed (BM/BP) (*p*-value<0.01; FDR<0.01; LogFC>1.5), after being normalized to the expression of count-per-million (CPM). The blue and red colors indicate a down-regulated and an up-regulated pattern, respectively.

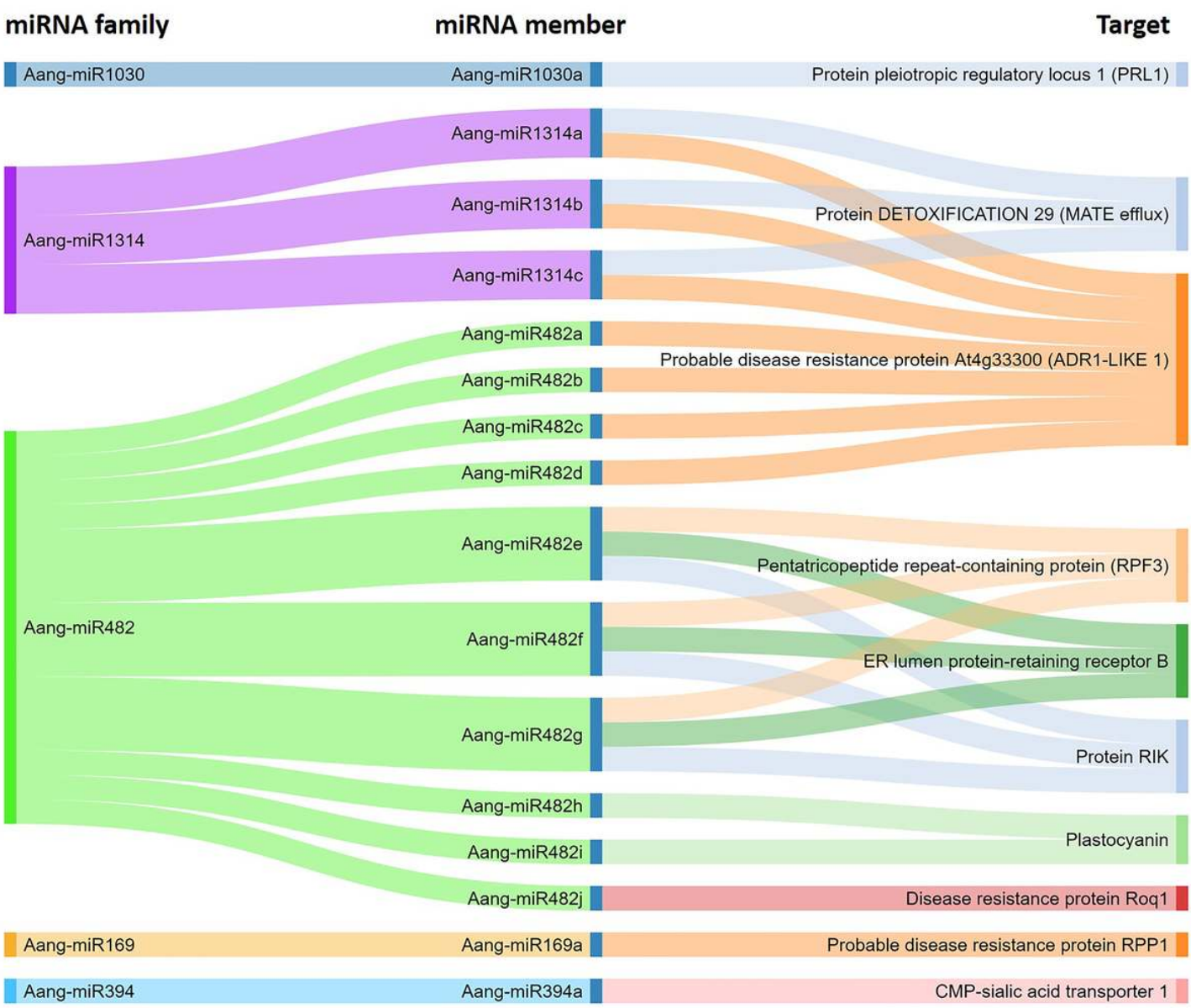

Figure 9

Sankey diagram of conserved miRNAs and their target genes. Targets were predicted by the psRNAtarget tool using an expectation cut-off of 2.5 and Trinotate v.3.2.1 pipeline. Complete information is available in Supplementary Tables S5 and S6.

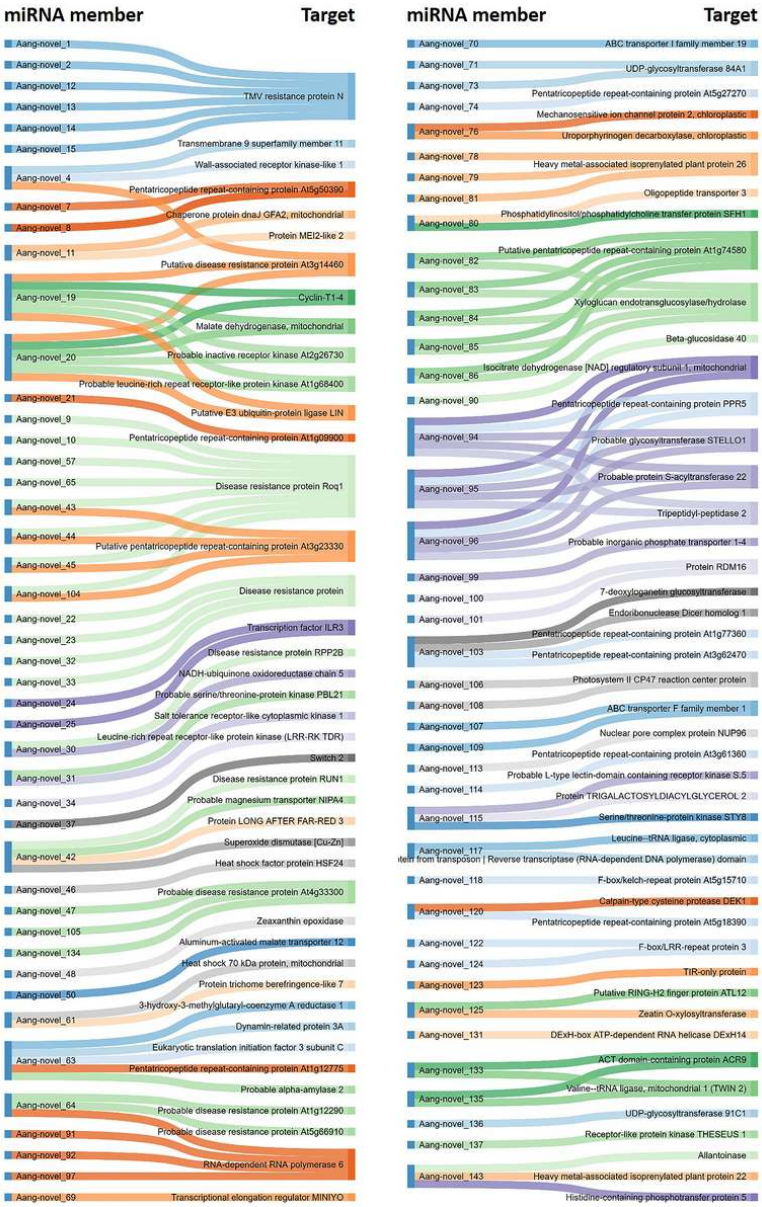

Figure 10

Sankey diagram of novel miRNAs and their target genes. Targets were predicted by the psRNAtarget using an expectation cut-off of 2.5 and Trinotate v.3.2.1 pipeline. Complete information is available in Supplementary Tables S5 and S6.

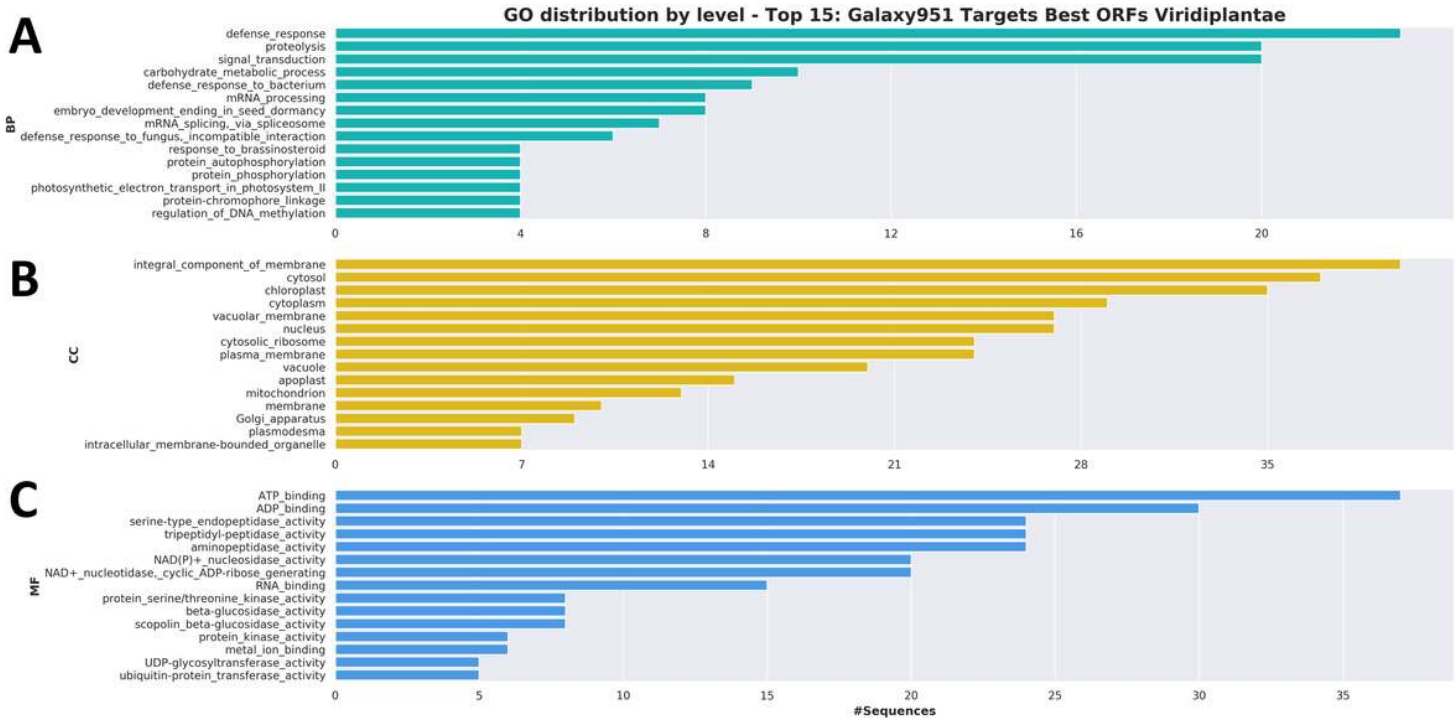

Figure 11

Gene Ontology (GO) classification of targets of conserved and novel miRNAs identified in this study. (A) Cellular component, (B) molecular function, and (C) biological process.

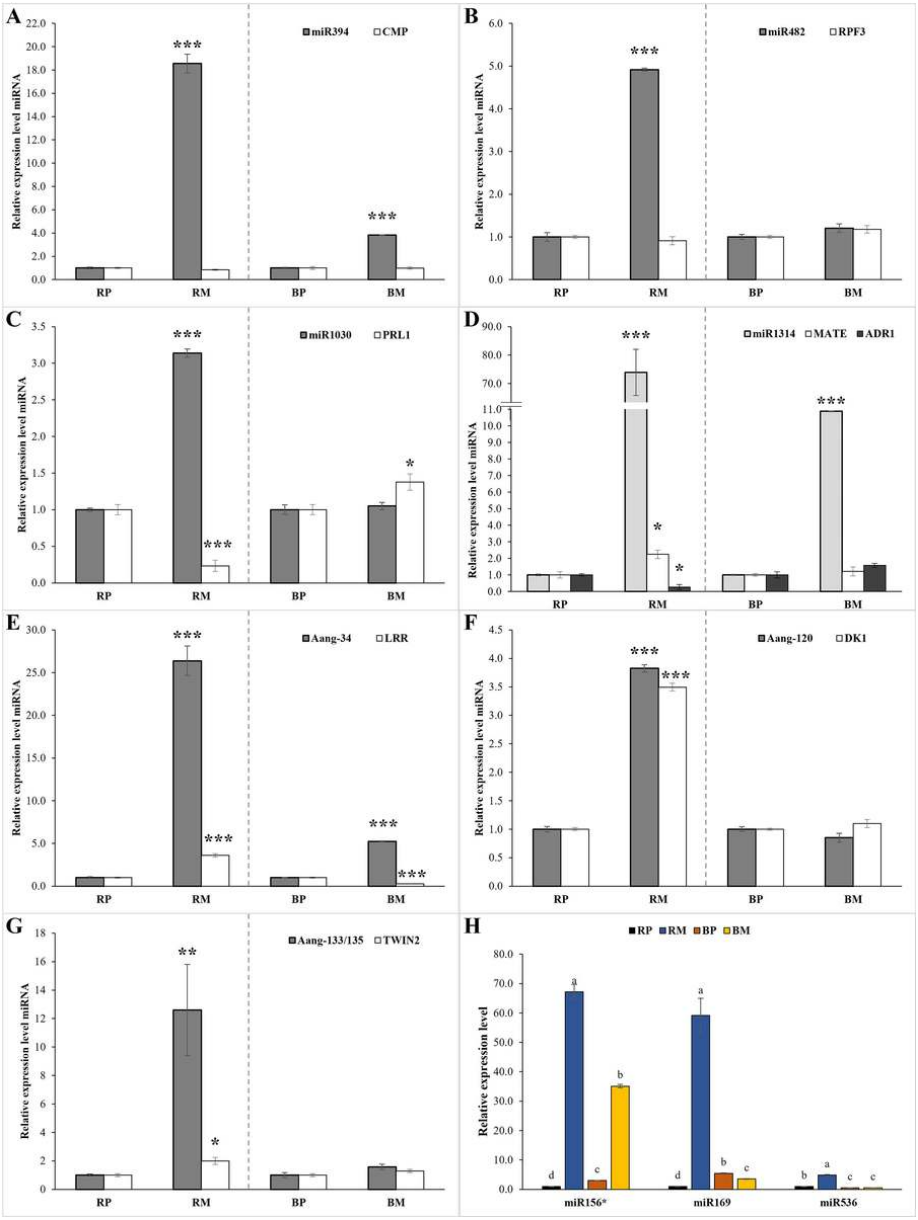

Figure 12

RT-qPCR expression profile of selected differentially regulated miRNAs and their target genes involved in somatic embryogenesis stages in two contrasting *Araucaria angustifolia* cell lines. RP, responsive cell line during proliferation stage; BP, blocked cell line during proliferation stage; RM, responsive during maturation stage; and BM, blocked during the maturation stage. miRNAs which targets could not be identified are presented in Fig. H. Expression values of miRNAs are represented as columns and target genes as continuous lines. Bars represent means ± standard error of three biological replicates. Significant differences among proliferation-maturation transition at a given cell line are indicated by asterisk (* $P<0.05$, ** $P<0.01$, *** $P<0.001$). In Fig. H, significant differences ($P<0.01$) among samples are indicated by letters, according to Tukey's test.

Supplementary Files

This is a list of supplementary files associated with this preprint. Click to download.

- Table1.docx
- SupplExcelFileE1.xlsx
- SupplExcelFileE2.xlsx
- SupplExcelFileE3.xlsx

- SupplementaryFileF1.pdf
- SupplementaryFileF2.pdf
- Supplementarymaterial.docx
- SupplementaryMaterialLegends.docx